Anti-*Acanthamoeba* activity of a semi-synthetic mangostin derivative and its ability in removal of *Acanthamoeba triangularis* WU19001 on contact lens

Julalak Chuprom [1, 2], **Suthinee Sangkanu** [1], **Watcharapong Mitsuwan** [3], **Rachasak Boonhok** [4], **Wilawan Mahabusarakam** [5], **L Ravithej Singh** [6, 7], **Ekachai Dumkliang** [8], **Kritamorn Jitrangsri** [9], **Alok K. Paul** [10], **Sirirat Surinkaew** [11], **Polrat Wilairatana** [12], **Maria de Lourdes Pereira** [13, 14], **Mohammed Rahmatullah** [15], **Christophe Wiart** [16], **Sonia Marlene Rodrigues Oliveira** [13, 17], **Veeranoot Nissapatorn** [Corresp. 1]

[1] School of Allied Health Sciences, Walailak University, Southeast Asia Water Team (SEA Water Team) and World Union for Herbal Drug Discovery (WUHeDD), and Research Excellence Center for Innovation and Health Products (RECIHP), Nakhon Si Thammarat 80160, Thailand

[2] School of Languages and General Education (SOLGEN), Walailak University, Nakhon Si Thammarat 80160, Thailand

[3] Akkhraratchumari Veterinary College, Walailak University, Nakhon Si Thammarat 80160, Thailand

[4] Department of Medical Technology, School of Allied Health Sciences, Walailak University, Research Excellence Center for Innovation and Health Products (RECIHP), Nakhon Si Thammarat 80160, Thailand

[5] Division of Physical Science, Faculty of Science, Prince of Songkla University, Songkhla 90110, Thailand

[6] Fluoro-Agrochemicals Division, CSIR – Indian Institute of Chemical Technology, Tarnaka, Hyderabad 500007, India

[7] Chemical Sciences Division, Academy of Scientific and Innovative Research, Ghaziabad 201002, India

[8] Faculty of Pharmacy, Silpakorn University, Pharmaceutical Development of Green Innovations Group (PDGIG), Nakhon Pathom 73000, Thailand

[9] Department of Pharmaceutical Chemistry, Faculty of Pharmacy, Silpakorn University, Nakhon Pathom 73000, Thailand

[10] School of Pharmacy and Pharmacology, University of Tasmania, Hobart, TAS 7001, Australia

[11] Department of Medical Technology, School of Allied Health Sciences, Walailak University, Nakhon Si Thammarat 80160, Thailand

[12] Department of Clinical Tropical Medicine, Faculty of Tropical Medicine, Mahidol University, Bangkok 10400, Thailand

[13] CICECO-Aveiro Institute of Materials & Department of Medical Sciences, University of Aveiro, 3810-193 Aveiro, Portugal

[14] Department of Medical Sciences, University of Aveiro, 3810-193 Aveiro, Portugal

[15] Department of Biotechnology & Genetic Engineering, Universiti Malaysia Sabah, Lalmatia, Dhaka 1207, Bangladesh

[16] The Institute for Tropical Biology and Conservation, Jalan UMS, Kota Kin-abalu, Sabah 88400, Malaysia

[17] Hunter Medical Research Institute, New Lambton, 2305 NSW, Australia

Corresponding Author: Veeranoot Nissapatorn
Email address: nissapat@gmail.com

Garcinia mangostana L., also known as the mangosteen tree, is a native medicinal plant in Southeast Asia having a wide variety of pharmacologically active compounds, including xanthonoid mangostin. In this study, we examined the pharmacological activities of the selected semi-synthetic mangostin derivative, namely, amoebicidal activity, encystation inhibition, excystation activity, and removal capacity of adhesive *Acanthamoeba* from the surface of contact lens (CL). Among the three derivatives, C1 exhibited promising anti-*Acanthamoeba* activity against *Acanthamoeba triangularis* WU19001 trophozoites and cysts. SEM images displayed morphological changes in *Acanthamoeba* trophozoites, including the loss of acanthopodia, pore formation in the cell membrane, and membrane damage. In addition, the treated cyst was shrunken and adopted an irregular flat cyst

shape. Under a fluorescence microscope, acridine orange and propidium iodide (AO/PI) staining revealed C1 induced condensation of cytoplasm and chromatin with the loss of cell volume in the treated trophozoites, while calcofluor white staining demonstrated the leakage of cell wall in treated cysts, leading to cell death. Interestingly, at the concentration ranges in which C1 showed the anti-*Acanthamoeba* effects (IC_{50} values ranging from 0.035-0.056 mg/mL), they were not toxic to Vero cells. C1 displayed the highest inhibitory effect on *A. triangularis* encystation at 1/16xMIC value (0.004 mg/mL). While C1 demonstrated the excystation activity at 1/128xMIC value with a high rate of 89.47%. Furthermore, C1 exhibited the removal capacity of adhesive *Acanthamoeba* from the surface of CL comparable with commercial multipurpose solutions (MPSs). Based on the results obtained, C1 may be a promising lead agent to develop a therapeutic for the treatment of *Acanthamoeba* infections and disinfectant solutions for CL.

1   **Anti-*Acanthamoeba* activity of a semi-synthetic mangostin derivative and its ability in**

2   **removal of *Acanthamoeba triangularis* WU19001 on contact lens**

4   Julalak Chuprom[1,2], Suthinee Sangkanu[1], Watcharapong Mitsuwan[3], Rachasak Boonhok[4],

5   Wilawan Mahabusarakam[5], L Ravithej Singh[6,7], Ekachai Dumkliang[8], Kritamorn Jitrangsri[9],

6   Alok K. Paul[10], Sirirat Surinkaew[11], Polrat Wilaratana[12], Maria L. Pereira[13,14], Mohammed

7   Rahmatullah[15], Christophe Wiart[16], Sonia Marlene Rodrigues Oliveira[13,17], Veeranoot

8   Nissapatorn[1]

10   [1] School of Allied Health Sciences, Southeast Asia Water Team (SEA Water Team) and World

11   Union for Herbal Drug Discovery (WUHeDD), and Research Excellence Center for Innovation

12   and Health Products (RECIHP), Walailak University, Nakhon Si Thammarat 80160, Thailand

13   [2] School of Languages and General Education (SOLGEN), Walailak University, Nakhon Si

14   Thammarat 80160, Thailand

15   [3] Akkhraratchumari Veterinary College, Walailak University, Nakhon Si Thammarat 80160,

16   Thailand

17   [4] Department of Medical Technology, School of Allied Health Sciences and Research Excellence

18   Center for Innovation and Health Products (RECIHP), Walailak University, Nakhon Si

19   Thammarat 80160, Thailand

20   [5] Department of Chemistry, Faculty of Science, Prince of Songkla University, Hat Yai, Songkhla

21   90112, Thailand

22   [6] Fluoro-Agrochemicals Division, CSIR – Indian Institute of Chemical Technology, Tarnaka,

23   Hyderabad 500007, India

24 [7] Chemical Sciences Division, Academy of Scientific and Innovative Research, Ghaziabad

25 201002, India

26 [8] Pharmaceutical Development of Green Innovations Group (PDGIG), Faculty of Pharmacy,

27 Silpakorn University, Nakhon Pathom 73000, Thailand

28 [9] Department of Pharmaceutical Chemistry, Faculty of Pharmacy, Silpakorn University, Nakhon

29 Pathom 73000, Thailand

30 [10] School of Pharmacy and Pharmacology, University of Tasmania, Hobart, TAS 7001, Australia

31 [11] Department of Medical Technology, School of Allied Health Sciences, Walailak University,

32 Nakhon Si Thammarat 80160, Thailand

33 [12] Department of Clinical Tropical Medicine, Faculty of Tropical Medicine, Mahidol University,

34 Bangkok 10400, Thailand

35 [13] CICECO-Aveiro Institute of Materials & Department of Medical Sciences, University of

36 Aveiro, 3810-193 Aveiro, Portugal

37 [14]Department of Medical Sciences, University of Aveiro, 3810-193 Aveiro, Portugal

38 [15] Department of Biotechnology & Genetic Engineering, University of Development Alternative,

39 Lalmatia, Dhaka 1207, Bangladesh

40 [16] The Institute for Tropical Biology and Conservation, Universiti Malaysia Sabah, Jalan UMS,

41 Kota Kin-abalu, Sabah 88400, Malaysia

42 [17] Hunter Medical Research Institute, New Lambton, 2305 NSW, Australia

44 **Corresponding author:**

45 Veeranoot Nissapatorn[1]

46 School of Allied Health Sciences, Walailak University, Nakhon Si Thammarat 80160, Thailand

47   E-mail: nissapat@gmail.com OR veeranoot.ni@wu.ac.th

49   **Abstract**

50   *Garcinia mangostana* L., also known as the mangosteen tree, is a native medicinal plant

51   in Southeast Asia having a wide variety of pharmacologically active compounds, including

52   xanthonoid mangostin. In this study, we examined the pharmacological activities of the selected

53   semi-synthetic mangostin derivative, namely, amoebicidal activity, encystation inhibition,

54   excystation activity, and removal capacity of adhesive *Acanthamoeba* from the surface of contact

55   lens (CL). Among the three derivatives, C1 exhibited promising anti-*Acanthamoeba* activity

56   against *Acanthamoeba triangularis* WU19001 trophozoites and cysts. SEM images displayed

57   morphological changes in *Acanthamoeba* trophozoites, including the loss of acanthopodia, pore

58   formation in the cell membrane, and membrane damage. In addition, the treated cyst was

59   shrunken and adopted an irregular flat cyst shape. Under a fluorescence microscope, acridine

60   orange and propidium iodide (AO/PI) staining revealed C1 induced condensation of cytoplasm

61   and chromatin with the loss of cell volume in the treated trophozoites, while calcofluor white

62   staining demonstrated the leakage of cell wall in treated cysts, leading to cell death. Interestingly,

63   at the concentration ranges in which C1 showed the anti-*Acanthamoeba* effects (IC_{50} values

64   ranging from 0.035-0.056 mg/mL), they were not toxic to Vero cells. C1 displayed inhibitory

65   effect of 9% on *A. triangularis* encystation at $1/16 \times MIC$ value (0.004 mg/mL). The excystation

66   activity was induced by lower C1 concentrations reaching 89.47% at $1/128 \times MIC$ value.

67   Furthermore, C1 exhibited the removal capacity of adhesive *Acanthamoeba* from the surface of

68   CL comparable with commercial multipurpose solutions (MPSs). Based on the results obtained,

69   C1 may be a promising lead agent to develop a therapeutic for the treatment of *Acanthamoeba*

70   infections and disinfectant solutions for CL.

71

72   **Introduction**

73   The number of contact lens (CL) wearers is continually increasing, and has been

74   estimated at over 140 million CL users worldwide (*Harbiyeli et al., 2022*). Poor hygiene habits

75   when handling CL, for example, inadequate lens cleaning, exposure of contact lenses to

76   contaminated water, prolonged use, and sleeping with CL, can lead to an increased risk of

77   developing infections keratitis (IK), which subsequently causes several clinical outcomes such as

78   corneal melting and scarring, ocular morbidity, scleral inflammation, and blindness (*Cope et al.,*

79   *2017*). A wide range of microorganisms can cause IK, for example, filamentous fungi (*Fusarium*

80   spp. and *Aspergillus* spp.), bacteria (*Pseudomonas aeruginosa*, *Staphylococcus aureus*,

81   *Streptococci* spp., *Enterobacteriaceae* spp., *Corynebacterium* spp., and *Propionibacterium* spp.),

82   viruses, and protozoa (*Acanthamoeba* spp.) (*O'Callaghan et al., 2019*; *Lee et al., 2021*; *Ting et*

83   *al., 2021*).

84   *Acanthamoeba* spp., opportunistic unicellular eukaryotic organisms, are free-living

85   amoeba (FLA) that reside in a remarkably wide range of habitats, including soil, air, and water

86   (*Lacerda & Lira, 2021*). They can be found in various water sources, for example, pond water,

87   swimming pools, beaches, tap water, and bottled water *(Esboei et al., 2020*; *Lacerda & Lira,*

88   *2021*). *Acanthamoeba* spp. can cause rare and fatal brain infections, commonly known as

89   granulomatous amoebic encephalitis (GAE) (*Sarink et al., 2022*). The mortality rate associated

90   with GAE exceeds 90% and occurs mainly among individuals with metabolic, physiological, and

91   immunological disorders or deficiencies (*Kalra et al., 2020*). *Acanthamoeba* can also cause

92   corneal infections and blindness, known as *Acanthamoeba keratitis* (AK), which is a sporadic

93   disease often related to CL users, and the incidence is increasing in many countries, including the

94   United States (*Maycock & Jayaswal, 2016*), New Zealand (*McKelvie et al., 2018*), and Denmark

95   (*Nielsen et al., 2020*). *Acanthamoeba* has only two life cycle stages, transforming from an active

96   form (trophozoite) to a dormant form (cyst) (*Fanselow et al., 2021*). The trophozoite is about 15-

97   50 μm in size and appears irregular, oval, round, or pear-shaped with spine-like structures known

98   as acanthopodia on its surface, which have been reported to show the ability to adhere to contact

99   lenses (*Lacerda & Lira, 2021*). *Acanthamoeba* transforms into a form of resistant cyst in harsh

100 environments or conditions, such as starvation, exposure to biocides or extreme temperatures,

101 pH, presence of chlorine, and changes in osmolarity (*Bergmanson et al., 2011*). The most

102 routinely used anti-*Acanthamoeba* keratitis drugs are antiseptics chlorhexidine (CHX) and

103 polyhexamethylene biguanide (PHMB). These drugs interact with the cytoplasmic membrane,

104 causing the loss of cellular components. They also inhibit enzymes that are necessary for cell

105 respiration (*Lorenzo-Morales, Khan & Walochnik, 2015*; *Fanselow et al., 2021*). However, the

106 potential toxicity of PHMB on human corneal cells has been reported (*Lorenzo-Morales et al.,*

107 *2013*). Therefore, the effort to develop safe and effective drugs remains a great challenge.

108   Various plants have been reported as an important source of amoebicidal agents against

109 *Acanthamoeba* infection with high anti-amoebic activity and low toxicity (*Niyyati, Dodangeh &*

110 *Lorenzo-Morales, 2016*). *Garcinia mangostana* L. (mangosteen, *Clusiaceae*) is a native of

111 Southeast Asia. It has been used as a medicinal plant (*Nauman & Johnson, 2022*). Mangosteen

112 pericarp (MP) is an important source of bioactive xanthones, which has remarkable antioxidant,

113 anti-inflammatory, immunomodulatory, antiviral, antifungal, antibacterial, and anticancer

114 activities (*Abate et al., 2022*; *Nauman & Johnson, 2022*). In literature, *G. mangostana* extract

115 and α-mangostin have previously shown anti-*Acanthamoeba* activity and anti-adhesion

116 properties against *Acanthamoeba triangularis* (*Sangkanu et al., 2021*; *Sangkanu et al., 2022*). In

117 this study, mangostin isolated from the pericarps of *G. mangostana* was modified to three semi-

118 synthetic derivatives using epoxidation and nitrile-addition reactions. The epoxy- and nitrile-

119 mangostin derivatives have gained more interest due to the discovery of anti-parasitic activity

120 against *Plasmodium falciparum* (*Mahabusarakam et al., 2006*) and antioxidant activity

121 (*Mahabusarakam et al., 2009*). The pharmacological activities of these compounds named 1,3-

122 dihydroxy-6-(2,3-epoxypropoxy)-7-methoxy-2,8-bis(3-methybut-2-enyl)-9H xanthen-9-one

123 (C1), 1-Hydroxy-3,6-di(4-cyanopropoxy)-7-methoxy-2,8-bis(3-methylbut-2-enyl)-9H xanthen-9-

124 one (C2), and 1,3-Dihydroxy-6-(4-cyanopropoxy)-7-methoxy-2,8-bis(3-methylbut-2-enyl)-9H-

125 xanthen-9-one (C3) were investigated. To our knowledge, these semi-synthetic compounds have

126 never been reported on anti-*Acanthamoeba* activities. This study, therefore, aims to (i) screen the

127 anti-*Acanthamoeba* activity of mangostin derivatives, (ii) evaluate the inhibition of

128 *Acanthamoeba* encystation and excystation activity of selected mangostin derivative, and (iii)

129 estimate the effect of the selected compound on the adhesion of *Acanthmoeba* to the surface of

130 contact lens (CL). These studies may provide more insights into the information of this selected

131 compound and future therapeutic applications related to *Acanthamoeba* infection or CL wearer.

132

133 **Materials & methods**

134 **Chemicals used**

135   Proteose peptone, Page's Saline, and yeast extract were procured from HiMedia

136 Laboratories (Mumbai, India). Sodium citrate dihydrate ($C_6H_5Na_3O_7.2H_2O$), disodium phosphate

137 ($NaHPO_4$), sodium chloride (NaCl), calcium chloride ($CaCl_2$), glucose, and

138   phenylmethylsulphonyl fluoride (PMSF) were from Sigma Chemical Co. (St. Louis, MO, USA).

139   Potassium dihydrogen phosphate (KH_2PO_4) and magnesium sulfate heptahydrate ($MgSO_4.7H_2O$)

140   were procured from Labscan (Bangkok, Thailand). Trypan blue (0.4%) was obtained from Gibco

141   BRL (Grand Island, NY, USA). All chemicals and medium components used were of analytical

142   grade.

143

144   **Preparation of mangostin and its derivatives**

145   The extraction and isolation procedures of mangostin were previously described by

146   *Mahabusarakam et al.* (*2009*). Briefly, 4 kg of air-dried powdered pericarps of *G. mangostana*

147   (*Mahabusarakam et al., 2009*) were soaked in 2.0 L of dichloromethane (CH_2Cl_2) for 48 h. The

148   extraction was repeated twice, and the combined solution was filtered through Whatman No. 1

149   filter paper (GE Healthcare Life Science, Buckinghamshire HP7 9NA, United Kingdom) using a

150   vacuum and pressure pump. The collected filtrate was evaporated to dryness under a vacuum at

151   45 °C using a rotary evaporator (Hei-VAP Advantage HL/G3, Heidolph, Schwabach, Germany).

152   The yellow precipitate was collected. The solid was re-dissolved in dichloromethane and

153   partitioned with 20% (w/v) sodium carbonate solution. The organic layer was separated and

154   washed with water several times until the water layer was no longer basic. The dried organic

155   layer was concentrated, and mangostin was obtained as a yellow crystalline solid.

156   To prepare epoxide derivative, a mixture of mangostin (5 g, 12 mmol) in

157   dimethylformamide (DMF) (20 mL) and sodium hybrid (2 g) in DMF (10 mL) was stirred at

158   room temperature for 30 min, followed by the addition of 2.5 mL 1-chloro-2,3-epoxypapane.

159   The reaction mixture was then refluxed for 6 h and worked up. The residue was purified by silica

160   gel chromatography and eluted with light petroleum/dichloromethane (4:5) to obtain 1,3-

161   Dihydroxy-6-(2,3-epoxypropoxy)-7-methoxy-2,8-bis(3-methylbut-2-enyl)-9H-xanthen-9-one

162   (C1) (1.5g, 26% yield) (*Mahabusarakam et al., 2006*).

163   The preparation of nitrile derivatives was previously described by *Mahabusarakam et al.*

164   (*2009*). A solution of mangostin (2 g, 4.8 mmol) in DMF (10 mL) and sodium hydride (2 g) in

165   DMF (5 mL) was stirred at room temperature for 30 min, followed by addition of 4-

166   chlorobutyronitrile (1.5 mL, 15 mmol). The reaction mixture was then refluxed for 5 h, poured

167   into iced water, neutralized with 3 M hydrochloric acid (HCl), and extracted with

168   dichloromethane. Later, the dichloromethane layer was washed with water and dried over

169   sodium sulfate. The solvent was removed, and the residue was purified by silica gel

170   chromatography. The sample was eluted with the mixed solvent of hexane/dichloromethane (1:8)

171   to give yellow needles of 1-Hydroxy-3,6-di(4-cyanopropoxy)-7-methoxy-2,8-bis(3-methylbut-2-

172   enyl)-9H-xanthen-9-one (C2) (1 g, 43% yield) and 1,3-Dihydroxy-6-(4-cyanopropoxy)-7-

173   methoxy-2,8-bis(3-methylbut-2-enyl)-9H-xanthen-9-one (C3) (0.25g, 9% yield).

174

175   **Strain and growth conditions**

176   *Acanthamoeba triangularis* WU19001 genotype T4 (MW647650) used in this study was

177   previously isolated from the recreational reservoir of Walailak University, Nakhon Si

178   Thammarat, Thailand, by *Mitsuwan et al.* (*2020*). The strain was seeded in T-25 tissue culture

179   flasks (SPL Life Science Co., Ltd., Gyeonggi-do, Korea) with 10 mL of peptone–yeast extract–

180   glucose (PYG) medium containing (g/L) proteose peptone 20, yeast extract 2.0 and glucose 18,

181    $C_6H_5Na_3O_7.2H_2O$ 1.0, $CaCl_2$ 0.059, $MgSO_4.7H_2O$ 0.98, sodium phosphate dibasic heptahydrate

182   ($Na_2HPO_4.7H_2O$) 0.355, KH_2PO_4 0.34, ammonium iron (II) sulfate hexahydrate

183   [Fe(NH$_4$)$_2$(SO$_4$)$_2$.6H$_2$O] 0.02 in 1000 mL distilled water pH 7.0. After incubation in a dark room

184   at ambient temperature for 72 h, *A. triangularis* trophozoites were observed.

185   For *A. triangularis* cyst preparation, the trophozoites grown in PYG medium for 72 h

186   were centrifuged at 4,000 rpm for 5 min in a Sorvall ST 40R centrifuge (Thermo Scientific, San

187   Jose, CA) and then washed twice with Neff's encystment medium pH 8.9 (*Neff et al., 1964*)

188   contained (g/L) KCl 7.455, ammediol [2-amino-2-methyl-1,3-propanediol 2.44, NaHCO$_3$ 0.084,

189   MgSO$_4$.7H$_2$O 1.968, CaCl$_2$.2H$_2$O 0.0588. The trophozoites were transferred into T-25 tissue

190   culture flasks containing 10 mL of an encystment medium, and encystation was induced in a

191   dark room at ambient temperature for 7 days. In order to obtain only mature cysts, the cells were

192   collected and then centrifuged at 4,000 rpm for 5 min and treated with sodium dodecyl sulfate

193   (SDS) solution at 0.5% (w/v) final concentration for 20 min to solubilize trophozoites and

194   immature cysts while mature cysts were resistant to SDS solution (*Moon et al., 2014*). Later, the

195   mature cysts were harvested by centrifugation at 4,000 rpm for 5 min and washed twice with

196   0.85% (w/v) NaCl solution. The obtained cysts were re-suspended in Neff's encystment medium.

197   The viability of *A. triangularis* trophozoites and cysts was determined by trypan blue

198   exclusion staining. *A. triangularis* suspension was mixed with the same volume of 0.2% trypan

199   blue and incubated at ambient temperature for 3 min (*Sangkanu et al., 2022*). The viable

200   (unstained) and dead (stained dark blue) amoebae were enumerated using a hemocytometer

201   (Tiefe Depth Profondeur, Marienfeld, Germany) under an inverted microscope (Nikon ECLIPSE

202   TE2000-S, Tokyo, Japan).

203

204   **Screening of anti-*Acanthamoeba* activity of mangostin derivatives**

205   Each of the compounds was screened for ant-*Acanthamoeba* activity against *A.*

206   *triangularis* trophozoites and cysts. Briefly, each of these compounds was dissolved in 100%

207   dimethyl sulfoxide (DMSO) to a 100 mg/mL final concentration and stored at -20 °C until use.

208   The stock solution of each compound was diluted with the cultivation medium to give the final

209   concentration of 2 mg/mL, and the 50 μL of aliquots were added to a 96-well plate (SPL Life

210   Sciences, Seoul, Korea). *A. triangularis* trophozoites and cysts were prepared as described

211   above, and an aliquot of 50 μL of cell suspension prepared at 2×10^5 cells/mL was inoculated into

212   each well of the plate, followed by incubation in a dark room at ambient temperature for 24 h.

213   The final concentration of DMSO was 1% (v/v), and medium containing 1% (v/v) DMSO was

214   used as a negative control, while a final concentration of 0.016 and 0.064 mg/mL chlorhexidine

215   (CHX) solution was used as a positive control for trophozoite and cyst, respectively. The trypan

216   blue exclusion staining was used to determine the number of viable cells present in samples as

217   described above.

218

219   **Determination of minimal inhibitory concentration (MIC) of mangostin derivatives**

220   The microtiter broth dilution method performed using a 96-well plate was used to

221   determine the MIC value of semi-synthesized compounds against *A. triangularis* trophozoites

222   and cysts according to the method of *Mitsuwan et al.* (*2020*). In this assay, each of the

223   compounds was diluted to give a final concentration of 0.016-1024 mg/mL. The cell suspension

224   was prepared as described above, after which 50 μL of an aliquot of the cell suspension (2×10^5

225   cells/mL) was seeded into each well and incubated at ambient temperature under darkness for 24

226   h. *A. triangularis* trophozoites and cysts exposed to 1% (v/v) DMSO and CHX solutions (a final

227   concentration of 0.008-0.128 mg/mL) were used as a negative and positive control, respectively.

228   The plates were incubated in a dark room at ambient temperature for 24 h. The viability was

229   calculated according to the following equation:

230   % Viability = (Mean of the viable parasite/Negative control) × 100

231   MIC is defined as the lowest concentration of the tested compound that inhibits visible

232   growth of at least 90% of *A. triangularis* (90% of amoeba died).

233

234   **Determination of inhibitory concentration 50 (IC$_{50}$)**

235   IC$_{50}$ of C1 and CHX against *Acanthamoeba* trophozoites and cysts was further

236   determined. The protocol was modified from *Kolören et al. (2019)*. In brief, the assay was

237   performed in a 96-well plate. C1 and CHX were prepared with two-fold serial dilution (a final

238   concentration of 0.015-1 mg/mL). Then, 50 µL of 2×10^5 cells/mL of trophozoites and cysts were

239   added to each well and incubated in a dark room at ambient temperature for 24 h. The untreated

240   parasite [medium containing 1% (v/v) DMSO] was included as a negative control. After

241   incubation for 24 h, trypan blue staining was used to determine the number of viable trophozoites

242   and cysts by counting on a hemocytometer. The results are given as percent inhibition compared

243   to control cells (considered as 100%). The IC$_{50}$ was calculated using the GraphPad Prism,

244   version 7 for Windows (GraphPad Software, CA, USA). This experiment was performed in

245   triplicate.

246

247   **Scanning electron microscopy (SEM) analysis**

248   *A. triangularis* trophozoites and cysts treated with C1 were carried out to observe any

249   morphological changes using SEM (Zeiss, Munich, Germany) at the Center for Scientific and

250   Technological Equipment, Walailak University, Nakhon Si Thammarat, Thailand (*Mitsuwan et*

251   *al., 2020*). The trophozoites were treated with 0.064 mg/mL C1 (1/2×MIC) and CHX 0.008

252   mg/mL (1/2×MIC). *A. triangularis* cysts were also treated with CHX (0.032 mg/mL) and C1

253   (0.032 mg/mL) at 1/2×MIC of CHX. After incubation in a dark room at ambient temperature for

254   24 h, cells were collected by centrifugation at 4,000 rpm for 5 min and washed three times in

255   0.01 M phosphate-buffered saline (PBS) solution pH 7.4. Cells were then smeared very thinly

256   onto a sterile cover glass and air-dried. The dried cover glass was placed in a 24-well plate and

257   fixed with 2.5% glutaraldehyde solution overnight at ambient temperature. The samples were

258   then washed three times with PBS solution and dehydrated in a graded series of ethanol solutions

259   from low- to high-density (20, 40, 60, 80, 90, and 100%) for 30 min at each step, further

260   mounted on aluminum stubs, and allowed to dry using a critical point dryer. The morphology of

261   *A. trianguaris* trophozoites and cysts was subsequently analyzed under SEM.

262

263   **Fluorescence microscopy by acridine orange and propidium iodide staining**

264   *A. triangularis* cell death after exposure to C1 was identified by AO/PI (acridine

265   orange/propidium iodide) double-staining assay according to the modified method of *Kusrini et*

266   *al.* (*2020*). For the staining, *A. triangularis* trophozoites were treated with CHX (0.008 mg/mL)

267   and C1 (0.064 mg/mL) at 1/2×MIC in 1.5 mL microcentrifuge tubes, followed by mixing. After

268   incubation for 24 h, samples were centrifuged at 4,000 rpm for 5 min, and the supernatant was

269   discarded and the pellet was washed twice with 0.01 M PBS solution pH 7.4. The pellets were

270   re-centrifuged at 4,000 rpm for 5 min and re-suspended in 100 μL AO/PI staining solution,

271   which was prepared by adding 200 μL of AO (1 mg/mL) and 200 μL PI (1 mg/mL) (Sigma

272   Chemical Co., St. Louis, MO, USA) in 600 μL 0.01 M PBS solution pH 7.4. The cell suspension

273   was then incubated in a dark room at ambient temperature for 10 min since both dyes are light-

274 sensitive and placed onto a slide, carefully covered with a coverslip. The cells were visualized

275 using a fluorescent microscope (Leica TCS SP5 laser scanning confocal microscope, Leica

276 microsystem Inc., Wetzlar, Germany). Live cells turned into green (AO), whereas the dead

277 appeared red (PI).

278

279 **Calcofluor White staining**

280   *A. triangularis* cysts were incubated in the absence or presence of C1 at $1/2 \times$ MIC (0.032

281 mg/mL) for 24 h. The cysts were harvested by centrifugation at 4,000 rpm for 5 min and washed

282 twice with 0.01 M PBS solution pH 7.4. *A. triangularis* cysts were re-suspended in 2.5%

283 calcofluor white (CFW) staining solution (Sigma Chemical Co., St. Louis, MO, USA) and

284 incubated in a dark room at ambient temperature for 120 min and collected by centrifugation at

285 4,000 rpm for 5 min. Later, it was washed twice with 0.01 M PBS solution pH 7.4 to remove

286 excess CFW stain and re-suspended in the same buffer solution. Finally, 20 μL cyst suspensions

287 were placed onto a slide, carefully covered with a coverslip, and examined under Olympus, BX-

288 53 fluorescent microscope (Olympus, Tokyo, Japan) with the excitation of 405 nm and emission

289 band pass 420-480 nm.

290

291 **Cytotoxicity assay**

292   The *in vitro* cytotoxicity of C1 and CHX was evaluated against the Vero cell

293 (Elabscience, Wuhan, Hubei, China) according to the method of *Eawsakul et al. (2017)*. Vero

294 cells were maintained in Dulbecco's Modifed Eagle's (DMEM) medium (Merck KGaA,

295 Darmstadt, Germany) supplemented with 10% (v/v) fetal bovine serum (FBS) and 1% antibiotic

296 cocktail containing penicillin G of 100 units/mL and streptomycin of 100 μg/mL. The culture

297   was incubated at 37 °C in a humidified 5% (v/v) CO_2 95% air atmosphere. The medium was

298   changed every 2 days until 90% confluence was achieved. The cells were then enzymatically

299   detached from the T-flask by adding trypsin-ethylenediaminetetraacetic acid (EDTA) solution

300   (0.25% trypsin, 1 mM EDTA), and subsequently incubated at 37 °C in a humidified incubator

301   (Binder, Tuttlingen, Germany) containing 95% room air / 5% CO_2. After incubation, 100 μL of

302   the suspensions were seeded in 96-well plates at a density of 1×10^5 cells/well, and then 100 μL

303   of C1 and CHX at different concentrations was added. Positive and negative controls were

304   prepared by adding the same amount of 1% (v/v) Triton X-100 and 0.01 M PBS solution pH 7.4,

305   respectively. After incubation for 24 h, the cell viability of treated Vero cells was determined

306   using a 3-(4,5-dimethylthiazol-2-yl)-2,5-diphenyltetrazolium bromide (MTT) assay. The medium

307   was removed and cells were incubated with fresh medium containing 0.5 mg/mL of MTT for 4 h.

308   The formed formazan crystal was dissolved by adding 100 mL of DMSO. The absorbance was

309   measured using a microplate reader (Metertech M965, Taipei, Taiwan) at 570 nm. The cell

310   viability was calculated using the following equation. Based on ISO 10993-5 standard, the

311   percentage of cell viability above 80% are non-cytotoxic; within 80-60% weak; 60-40%

312   moderate, and below 40% strong cytotoxic, respectively (International Organization for

313   Standardization ISO 10993-5, 2009).

314   Cell viability (%) = (ABt/ABu)×100

315   ABt and ABu are the absorbance values of treated and untreated cells, respectively

316

317   **Effect of mangostin derivative on *A. triangularis* encystation**

318   The effect of C1 on *A. triangularis* encystation was assessed in 96-well plates according

319   to the modified method of *Fakae et al.* (*2020*). In brief, C1 was diluted with Neff's encystment

320 medium to give a final concentration of 1/2×MIC - 1/32×MIC. Then, 50 μL of each dilution

321 was added to each well, and an aliquot of 50 μL containing approximately 6×10^5

322 trophozoites/mL was seeded into each well of the 96-well plate. The trophozoites in the presence

323 of 10 mM phenylmethylsulfonyl fluoride (PMSF) were used as a positive control, whereas the

324 trophozoites exposed to an encystment medium containing 1% (v/v) DMSO served as a negative

325 control. The plates were incubated in a dark room at ambient temperature for 72 h. The viability

326 of *A. triangularis* cells was quantified by trypan blue exclusion staining using a hemocytometer.

327 To solubilize all trophozoites, a final concentration of 0.5% (w/v) SDS solution was added and

328 incubated at ambient temperature for 30 min with mild shaking, and cysts were enumerated

329 using a hemocytometer. The inhibition effect of mangostin derivative on encystation was

330 calculated according to the following equation:

331 Percentage of encystation inhibition = 100 - (Post-digestion number/Pre-digestion number)×100

332

333 **Effect of mangostin derivative on excystation activity of *A. triangularis***

334   The excystation assay was performed to determine the effect of C1 on excystation

335 activity of *A. triangularis*. The protocol for this assay was obtained from *Anwar et al.* (*2019*)

336 with a slight modification. C1 was diluted with a PYG growth medium to give a final

337 concentration of 1×MIC - 1/128×MIC. An aliquot of 50 μL of each dilution was added to each

338 well, and cell suspension containing 6×10^5 cysts/mL was prepared as described above and

339 followed by adding 50 μL of this into each well. The cysts in the presence of 10 mM PMSF were

340 served as a negative control, while the cysts without C1 exposure served as a positive control.

341 After incubation in a dark room at ambient temperature for 7 days (*Shing, Balen & Debnath,*

342 *2021*), a final concentration of 0.5% (w/v) SDS solution was added to solubilize all trophozoites

343   and incubated at ambient temperature for 30 min with mild shaking, and cysts were enumerated

344   using a hemocytometer. The excystation rate was calculated according to the following equation:

345   Excystation rate (%) = (No. of total cell - No. of cyst/No. of total cells)$\times$100

346   The results are representatives of three experiments presented as mean $\pm$ standard error.

347

348   **Effect of mangostin derivative on the adhesion of *A. triangularis* to the surface of contact**

349   **lenses (CL)**

350   The potential of C1 in removing *A. triangularis* trophozoites and cysts adherent to

351   contact lens (CL) was evaluated according to a previous study (*Mitsuwan et al., 2020*) with slight

352   modification. In this assay, the commercial CL-1 was removed from the original package and

353   placed in a 24-well plate. Each lens was rinsed twice with 0.01 M PBS solution pH 7.4. *A.*

354   *triangularis* trophozoites and cysts were prepared as described above, and an aliquot of 500 μL

355   cell suspension containing 1×10^6 cells/mL was dropped on the CL in a 24-well plate and

356   incubated in a dark room at ambient temperature for 24 h. C1 and CHX at a final concentration

357   of $1/2\times$MIC (500 μL) were added to each well and incubated at ambient temperature under

358   darkness for 24 h. Two brands of multi-purpose disinfecting (MPD) solutions, including

359   Renu®freshTM (Bausch & Lomb, USA) (MPD-1) and Duna NO RUB (Alcon laboratories, INC,

360   Fort Worth, USA) (MPD-2) were used as positive controls. Contact lenses (CL) were gently

361   washed with 0.01 M PBS solution pH 7.4 and transferred to a microcentrifuge tube. The samples

362   were then placed in an ice bath for 10 min and shaken in a vortex for 5 min. The total number of

363   cells in the microcentrifuge tube was counted under an inverted microscope.

364

365   **Statistical analysis**

366   All experiments were carried out in triplicate, and the mean values were registered. The

367   data were compared by one-way ANOVA and the Tukey's t-test using the statistical package

368   software (SPSS version 26.0, IL, Chicago, USA). Data were expressed as mean ± SD. In all

369   analyzes, $p < 0.05$ was considered statistically significant.

370

371   **Results**

372   **Effect of mangostin derivatives against *A. triangularis***

373   The anti-*Acanthamoeba* activity of the mangostin derivatives at a final concentration of

374   1.0 mg/mL against *A. triangularis* WU19001 trophozoites and cysts was screened through the

375   microtiter broth dilution method. Three semi-synthetic mangostin derivatives were obtained: 1,3-

376   Dihydroxy-6-(2,3-epoxypropoxy)-7-methoxy-2,8-bis(3-methylbut-2-enyl)-9H-xanthen-9-one

377   (C1, epoxide derivative), 1-Hydroxy-3,6-di(4-cyanopropoxy)-7-methoxy-2,8-bis(3-methylbut-2-

378   enyl)-9H xanthen-9-one (C2, nitrile derivative) and 1,3-Dihydroxy-6-(4-cyanopropoxy)-7-

379   methoxy-2,8-bis(3-methylbut-2-enyl)-9H-xanthen-9-one (C3, nitrile derivative), and their

380   chemical structures were shown in Fig. 1. These tested compounds exhibited inhibitory activities

381   at 1 mg/mL and were further evaluated for their MICs. Among these, C1 showed greater anti-

382   *Acanthamoeba* activity at 0.128 mg/mL and 0.064 mg/mL on trophozoites and cysts,

383   respectively (Table 1). Moreover, C1 exhibited anti-*Acanthamoeba* cysts activity similar as

384   chlorhexidine (CHX). Regarding to mangostin nitrile derivatives included C2 and C3 on *A.*

385   *triangularis* trophozoites and cysts, both exhibited much higher MIC values *in vitro* against

386   trophozoites (0.512 mg/mL) and cyst (>1 mg/mL) compared to those of CHX. C1 and CHX also

387   were shown in demonstrating the inhibitory activity against *Acanthamoeba* trophozoites with

388   IC$_{50}$ of 0.056 and 0.014 mg/mL, respectively (Fig. 2). In addition, C1 and CHX exhibited the

389   inhibitory effect against cysts with IC_{50} values of 0.035 and 0.038 mg/mL, respectively (Fig. 2).

390   In this regard, C1 was selected for further study.

391

392   **Effect of mangostin derivative on morphological changes of *A. triangularis***

393   The morphological changes of the *A. triangularis* trophozoites upon exposure to C1 at its

394    $1/2\times$MIC value (0.064 mg/mL) were observed by scanning electron microscopy (SEM). The *A.*

395   *triangularis* trophozoites exhibited spine-like structures on their surface known as acanthopodia.

396   Based on the SEM images, shortening and loss of acanthopodia on the amoeba membrane were

397   observed after treated trophozoites with C1 (0.064 mg/mL) (Fig. 3A) and CHX (Fig. 3D) for 24

398   h. Moreover, trophozoites treated with CHX at $1/2\times$MIC value (0.008 mg/mL) showed stronger

399   loss of acanthopodia compared to that of C1. On the contrary, untreated cells exhibited numerous

400   acanthopodia on the amoebic surface (Fig. 3G). The most remarkable changes on the amoeba

401   morphology after treated with C1 and CHX were the reduction of cell size, development of

402   abnormal shapes, blebbing on the plasma, pore formation in the cell membrane, and membrane

403   damage (Fig.3). A large number of pores were detected in treated trophozoites with CHX when

404   compared to those of C1.

405   SEM images displayed morphological changes in *A. triangularis* cysts treated with C1

406   ($1/2\times$MIC value = 0.032 mg/mL). In this condition, cysts became shrunk and showed thick

407   ridges on the wrinkled surface with the observation of flat and irregular shapes (Figs. 4A-C). The

408   normal morphological characteristics such as triangular shape, smooth surface, and appearance

409   of thin ridges on the wrinkled surface were observed in the untreated cysts (Figs. 4G-I). The cyst

410   size of treated ones with CHX at $1/2\times$MIC value (0.032 mg/mL) was smaller compared with

411 treated cysts with C1 (Figs. 4A and 4D). In addition, the result also showed that the cysts treated

412 with CHX had rougher surfaces compared to those treated with C1.

413

414 **Determination of cell death by fluorescence microscopy-acridine orange/ propidium iodide**

415 **(AOPI) staining**

416   AO/PI double staining is a technique used to differentiate between viable and non-viable

417 cells. In untreated trophozoites, the cells were observed the green cytoplasm and bright green

418 fluorescent of an intact nucleus stained by AO, indicating healthy and viable *Acanthamoeba* cells

419 (Fig. 5C). In addition, a prominent vacuole was seen in untreated *Acanthamoeba* trophozoite.

420 Meanwhile, *A. triangularis* cells treated with C1 and CHX were observed as orange to red

421 granules in cells, indicating non-viable *Acanthamoeba* cells (Figs. 5A-B).

422

423 **Detection of cysticidal activity by calcofluor white staining**

424   The cysticidal activity of C1 on *A. triangularis* cysts was evaluated by calcofluor white

425 (CFW) staining assay. This fluorescence stain is known to bind to the cellulose deposition in the

426 cell wall layer of *Acanthamoeba* cysts (*El-Sayed & Hikal, 2015*). The cell walls of

427 *Acanthamoeba* cyst consisting of two layers identified as ectocyst and endocyst were observed in

428 untreated cysts (Figs. 6A-B and E). Furthermore, our results showed that C1 and CHX had

429 cysticidal activities and caused cyst death based on the loss of CFW staining (Figs. 6C-D).

430

431 ***In vitro* cell cytotoxicity**

432   The cytotoxicity of C1 and CHX towards Vero cells was investigated using the MTT

433 assay. The IC_{50} values of C1 for *Acanthamoeba* trophozoites and cysts were 0.056 and 0.035

434   mg/mL, respectively. According to ISO 10993-5, at the cell viability exceeds 80%, compound is

435   considered non-cytotoxic, while at cell viability range between 60-80%, as weakly cytotoxic. In

436   this study, the non-cytotoxic dose of C1 was 0.04 mg/mL and the weakly cytotoxic concentration

437   of C1 was 0.08 mg/mL (Fig.7). Therefore, the results confirmed that C1 had no cytotoxic effect

438   on Vero cells at inhibitory concentrations. The IC_{50} values of CHX for *Acanthamoeba*

439   trophozoites and cysts were 0.014 and 0.038 mg/mL, respectively and this obtained data

440   indicated that CHX had strong cytotoxic effect on Vero cells.

441

442   **Effect of mangostin derivative as an inhibitor on *A. triangularis* encystation**

443   Encystation of *Acanthamoeba* leads to cyst formation from vegetative trophozoites. This

444   is essential for parasite survival under harsh conditions. The inhibitory effect of C1 on *A.*

445   *triangularis* encystation was evaluated. Based on the results obtained, C1 displayed a high

446   inhibitory effect on *A. triangularis* encystation at $1/2 \times$ MIC (0.064 mg/mL) to 1×32 MIC (0.008

447   mg/mL) with encystation inhibition of 6.0-9.0% (Fig. 8). Of this, the best encystation inhibition

448   was observed at $1/16 \times$ MIC (0.004 mg/mL) (Fig. 8). Meanwhile, 10 mM PMSF was used as a

449   positive control and suppressed up to 90% of trophozoites from forming into cysts (Fig. 8). C1

450   gave a better inhibitory effect against *A. triangularis* encystation compared to control group

451   (without C1) (Fig. 8).

452

453   **Effect of mangostin derivative on the excystation activity of *A. triangularis***

454   Excystation assay was conducted to determine the effect of C1 on the ability of *A.*

455   *triangularis* to re-emerge from the cyst stage to trophozoites. Cysts treated with PMSF (10 mM)

456   were used as a negative control, while the cysts without C1 exposure were used as a positive

457   control. According to the results, the treatment of amoebic cysts with C1 significantly succeeded

458   in triggering excystation ($p < 0.05$) at $1/128 \times$ MIC, as compared to the control groups (10 mM

459   PMSF and without adding C1) (Fig. 9) with excystation rate of 89.47%. In addition, treatment of

460   *A. triangularis* cysts with C1 at $1/2$-$1/8 \times$ MICs exhibited moderate efficiency for excystation

461   activity with excystation rate of 23 to 28% (Fig. 9). In our study, the incomplete excystment of

462   *A. triangularis* in PYG medium at an optimal 10 day period with the excystation rate of 100%

463   was found (Fig. 9).

464

465   **The ability of mangotsin derivative on the removal of adhesive *A. triangularis* trophozoites**

466   **and cysts on contact lenses (CL)**

467   The ability of C1 for the removal of adhesive *A. triangularis* trophozoites and cysts on

468   contact lenses (CL) was investigated. Two commercial multi-purpose disinfecting (MPD-1 and -

469   2) solutions and CHX were used as positive controls, while the CL without C1 exposure was

470   considered as a negative control. Our result showed that C1 had the greatest capability to remove

471   adherent *A. triangularis* trophozoites on CL compared to a negative control (Fig. 10A). In

472   addition, low numbers of trophozoites and cysts adherent on CL were observed in the presence

473   of C1, CHX, and both MPD-1 and-2 solutions (Figs. 10A-B). Therefore, C1 gave

474

475   **Discussion**

476   In the present study, the anti-*Acanthamoeba* of semi-synthetic mangostin derivatives was

477   evaluated *in vitro*. Natural products are important sources for developing new drugs or

478   supplementary products. In fact, the growing rate of *Acanthamoeba* infection causing keratitis

479   and the toxicity of some used medicines have been reported worldwide (*Arabaci et al., 2013*;

480   *Ortillés et al., 2017*). Therefore, the introduction of new agents is timely needed for an effective

481   treatment. Till date, there are scanty reports on the anti-*Acanthamoeba* activity of *Garcinia*

482   *mangostana extract* on *Acanthamoeba* (*Sangkanu et al., 2021*; *Sangkanu et al., 2022*). To the

483   best of our knowledge, C1 as the semi-synthetic mangostin (epoxide) derivative has the first ever

484   shown anti-*Acanthamoeba* activity against *A. triangularis* trophozoites (MIC and IC_{50} values of

485   0.128 and 0.056 mg/mL, respectively); this compound also exhibited a high amoebicidal activity

486   against cysts (MIC and IC_{50} values of 0.064 and 0.035 mg/mL, respectively) proving to be the

487   same effective as chlorhexidine (CHX). To support this, *Lorenzo-Morales et al. (2019)* reported

488   the IC_{50} values of semisynthetic substances of red alga *Laurencia viridis* named

489   dehydrothyrsiferol against *Acanthamoeba castellanii* Neff trophozoites and cysts. Additionally,

490   semi-synthetic α-mangostin derivatives also demonstrated high potential anti-bacterial and anti-

491   fungal activities *in vitro* (*Narasimhan et al., 2017*).

492   The present study clearly demonstrated the anti-*Acanthamoeba* activity of C1 supported

493   by SEM images of morphological changes in trophozoites, including the appearance of irregular

494   cell shapes, pore formation on the amoeba surface, and strong loss of the acanthopodia structure.

495   Similar effects were reported after treating *Acanthamoeba polyphaga* trophozoites with cationic

496   carbosilane dendrimers (*Heredero-Bermejo et al., 2015*). The acanthopodia are essential for host

497   cell adhesion and cellular movements. Adhesion of *A. triangularis* to contact lens (CL) via

498   acanthopodia could be one of the reasons supporting the amoeba transmission and infection in

499   the eyes (*Ahmed Khan, 2003*). The formation of pores on the amoebic surface after treating

500   trophozoites with C1 can lead to a leakage in the cytoplasmic content and death of the amoeba.

501   This phenotypic change is in agreement with *Heredero-Bermejo et al. (2020)*, which

502   demonstrated that the membrane alteration caused the *Acanthamoeba* cell death. Furthermore,

503   C1 exhibited the anti-*Acanthamoeba* activity towards *A. triangularis* cysts. This finding was

504   confirmed by SEM results of morphological changes, including loss of ridges, membrane

505   blebbing, and cell shrinkage. This shrinkage might be due to the detachment of the plasma

506   membrane from the endocyst (*Carrijo-Carvalho et al., 2017*). These morphological changes

507   might imply that the cysts were destroyed. A similar observation was reported after

508   *Acanthamoeba* spp. cysts were treated with *Aloe vera* ethanol extract and honey (*Kadry et al.,*

509   *2021*).

510   For acridine orange and propidium iodide (AO/PI) staining, AO is an intercalating dye

511   that can enter internal parts of *Acanthamoeba* through non-compromised membrane integrity and

512   is able to bind to nucleic acids, emits green fluorescent detecting live and dead cells, whereas, PI

513   can only enter dead cells with poor membrane integrity and red-orange fluorescence on the cells

514   (*Foglieni, Meoni & Davalli, 2001*). The exposed trophozoites with C1 at $1/2 \times$ MIC value and

515   stained with AO/PI dyes were observed as yellow-orange granules in cells. These fluorescence

516   granules are believed to be lysosomes, taking up the AO stain through the known sequestration

517   and digestion process of cytoplasmic macromolecules (*Kusrini et al., 2018*). *Acanthamoeba* cells

518   treated with CHX at $1/2 \times$ MIC value of 0.008 mg/mL exhibited phenotypic characteristics of red

519   nuclei and green cytoplasm, which indicated that they were non-viable cells. In contrast, the

520   untreated cells were visible as green fluorescence cells, indicating healthy cells with the intact

521   plasma membrane. The microscopy images revealed that the smaller size of the treated cells with

522   C1 and CHX, compared to those in the untreated cells indicated the condensation of the

523   chromatins. The similar observation in *Acanthamoeba* treated with acyclic and cyclic-samarium

524   complexes was also described by *Kusrini et al. (2018)*. In addition, the large vacuole was found

525   in untreated cell and *A. triangularis* cell size after exposure to C1 and CHX becomes smaller

526   compared to untreated cells. According to the result of *Nakisah et al. (2012)*, apoptosis was

527   found after treating *Acanthamoeba* cells with Malaysian marine sponge *Aaptos* sp. methanol

528   extract and stained with AO/PI technique. The condensation of cytoplasm and chromatin was

529   established with smaller cell size. Our result indicated that exposure to the cells with C1 and

530   CHX induced apoptosis in *Acanthamoeba*.

531   The present study used the calcofluor white (CFW) staining solution to distinguish

532   between live and dead cysts. This staining solution has a specific affinity for cellulose, a major

533   component of the *Acanthamoeba* cyst wall (*Marines, Osato & Font, 1987*). It indicated that the

534   cysts treated with C1 lose the CFW staining due to loss or leakage of the cell wall, leading

535   ultimately to cell death. This leakage may emanate from conformational changes and weakening

536   of the inter-fiber bonds of the cellulose cell wall (*Mooney et al., 2020*). In addition, the

537   cytotoxicity assay demonstrated that C1 was non-cytotoxic on Vero cells, whereas CHX

538   displayed a strong cytotoxic effect. CHX was found to be a cytotoxic agent to human

539   osteoblastic cell line (*Lee et al., 2010*), human dermal fibroblasts (*Hidalgo & Dominguez, 2001*),

540   and human alveolar bone cells (*Cabral & Fernandes, 2007*). Our results agree with previous

541   research in which CHX exhibited cytotoxic effect on Vero cells (*Baqui et al., 2001*).

542   Interestingly, it was found that C1 showed an effect on encystation inhibition.

543   Encystation of *Acanthamoeba* is the phenotypic transformation from vegetative trophozoites to

544   cysts which occurs under unfavorable conditions (*Chávez-Munguía et al., 2005*). C1 gave the

545   encystation inhibition of 9%, while it was not detected in the negative control (without adding

546   C1). In addition, C1 was effective in increasing excystation rate of up to 85% compared to the

547   negative control. In literature, the process of excystment consists of 5 stages: mature cyst,

548   activated cyst stage, early pre-emergence stage, late pre-emergence, and complete emergence

549 (*Mattar & Byers, 1971*). Excystment occurs when mature cysts are transferred from the

550 encystment medium (Neff's encystment medium) back into the growth medium that contains

551 proteose peptone, yeast extract and glucose (PYG medium). However, the time of

552 *Acanthamoeba* excystment processes depends upon species or conditions (e.g., pH, temperature,

553 and time duration) (*Mattar & Byers, 1971*; *Marciano-Cabral & Cabral, 2003*). In our study,

554 excystment of *A. triangularis* was completed within 10 days in PYG medium with the

555 excystation rate of 100%. Many proteases (cysteine, serine, and metal) are used for encystation

556 and excystation of protozoan parasites, including *Acanthamoeba* (*Lee et al., 2015*). PMSF is a

557 serine protease inhibitor that inhibits serine protease activity; therefore, encystation and

558 excystation were diminished in the presence of this inhibitor. According to the result, C1 may

559 stimulate the protease activity that leads to a high excystation rate in the presence of C1

560 compared to the control. Generally, *Acanthamoeba* trophozoites transform into a cyst form to

561 protect themselves under harsh conditions such as extreme temperatures, extreme pHs, and anti-

562 agents. In our study, we found that *Acanthamoeba* maintained themselves into cyst form under

563 high concentrations of C1 (1/2 to 1/8 MIC values) for survival against stress conditions;

564 therefore excystation rates were low. Whereas, at low concentrations of C1 (1/16 to 1/128 MIC

565 values), *Acanthamoeba* cysts transformed into trophozoites because the excystation activity was

566 induced. Based on our results, the concentrations of C1 can therefore be divided into three

567 categories: 1) MIC values for cyst destruction, 2) 1/2 to 1/8 MIC values for inhibition of

568 excystation activity and 3) 1/16 to 1/128 MIC values for induction of excystation activity. These

569 C1 concentrations were of paramount importance for the development of future therapeutic

570 agents of *Acanthamoeba* infections.

571   In this study, we further found that C1 showed high efficiency in removing adhesive *A.*

572   *triangularis* trophozoites and cysts from CL surface. This may be due to a lack of acanthopodia

573   which is the main adhesive structure of trophozoites used for the surface attachment such as

574   contact lenses (*Sangkanu et al., 2022*). Moreover, *Acanthamoeba* cells change to irregularly

575   shaped cells and rounded trophozoites in response to the compound in order to protect

576   themselves from environmental conditions such as stress (*Boonhok et al., 2021*). Based on this

577   experiment, C1 is considered as a potential candidate for future studies mainly to demonstrate

578   the actual role of this compound against other pathogenic *Acanthamoeba* infections and to

579   explore the potential pharmaceutical applications in the future. Furthermore, the results obtained

580   in this study revealed that C1 showed high efficacy in removing adhesive *A. triangularis*

581   trophozoites and cysts from CL surface, which can be applied for lens care solution. In addition,

582   an assessment of additional pathogenic clinical strains of *Acanthamoeba* sp. (*e.g.*, *A. castellanii*

583   and *A. polyphaga*) is of paramount importance in our future studies.

584

585   **Conclusions**

586   Our study indicated that the mangostin derivative named 1,3-Dihydroxy-6-(2,3-

587   epoxypropoxy)-7-methoxy-2,8-bis(3-methylbut-2-enyl)-9H-xanthen-9-one (C1, epoxide

588   derivative) exhibited the potent anti-*Acanthamoeba* activities against *A. triangularis* trophozoites

589   and cysts. This compound showed ability in encystation inhibition and induced the

590   *Acanthamoeba* excystation activity. Furthermore, it is interesting to note that C1 exhibited high

591   potential on the removal of adhesive *A. triangularis* trophozoites and cysts from contact lenses

592   (CL). Our result suggests that C1 could be a potential source in the development of cleaning or

593   disinfecting solutions for contact lenses and a novel therapeutic agent against *Acanthamoeba*

594   infections in the future.

595

596   **References**

597   **Abate M, Pagano C, Masullo M, Citro M, Pisanti S, Piacente S, Bifulco M. 2022.**

598   Mangostanin, a xanthone derived from *Garcinia mangostana* fruit, exerts protective and

599   reparative effects on oxidative damage in human keratinocytes. *Pharmaceuticals* 15:84

600   DOI: 10.3390/ph15010084.

601   **Ahmed Khan N. 2003.** Pathogenesis of *Acanthamoeba* infections. *Microbial Pathogenesis*

602   34:277–285 DOI: 10.1016/S0882-4010(03)00061-5.

603   **Anwar A, Chi Fung L, Anwar A, Jagadish P, Numan A, Khalid M, Shahabuddin S,**

604   **Siddiqui R, Khan NA. 2019.** Effects of shape and size of cobalt phosphate nanoparticles

605   against *Acanthamoeba castellanii. Pathogens* 8:260. DOI: 10.3390/pathogens8040260.

606   **Arabaci T, Türkez H, Çanakçi CF, Özgöz M. 2013.** Assessment of cytogenetic and cytotoxic

607   effects of chlorhexidine digluconate on cultured human lymphocytes. *Acta Odontologica*

608   *Scandinavica* 71:1255–1260. DOI: 10.3109/00016357.2012.757646.

609   **Baqui A a. MA, Kelley JI, Jabra-Rizk MA, DePaola LG, Falkler WA, Meiller TF. 2001.** *In*

610   *vitro* effect of oral antiseptics on human immunodeficiency virus-1 and herpes simplex

611   virus type 1. *Journal of Clinical Periodontology* 28:610–616. DOI:

612   https://doi.org/10.1034/j.1600-051x.2001.028007610.x.

613   **Bergmanson JPG, Wang E, Gire AI, Osato MS. 2011.** *In vitro* effects of medium tonicity,

614   nutrient concentration, and free chlorine content on *Acanthamoeba. Contact Lens and*

615   *Anterior Eye* 34:164–168. DOI: 10.1016/j.clae.2011.02.003.

616   **Boonhok R, Sangkanu S, Chuprom J, Srisuphanunt M, Norouzi R, Siyadatpanah A,**

617   **Mirzaei F, Mitsuwan W, Wisessombat S, de Lourdes Pereira M, Rahmatullah M,**

618   **Wilairatana P, Wiart C, Ling LC, Dolma KG, Nissapatorn V. 2021.** *Peganum*

619   *harmala* extract has antiamoebic activity to *Acanthamoeba triangularis* trophozoites and

620   changes expression of autophagy-related genes. *Pathogens* 10:842. DOI:

621   10.3390/pathogens10070842.

622   **Cabral CT, Fernandes MH. 2007.** *In vitro* comparison of chlorhexidine and povidone-iodine

623   on the long-term proliferation and functional activity of human alveolar bone cells.

624   *Clinical Oral Investigations* 11:155–164. DOI: 10.1007/s00784-006-0094-8.

625   **Carrijo-Carvalho LC, Sant'ana VP, Foronda AS, de Freitas D, de Souza Carvalho FR.**

626   **2017.** Therapeutic agents and biocides for ocular infections by free-living amoebae of

627   *Acanthamoeba* genus. *Survey of Ophthalmology* 62:203–218 DOI:

628   10.1016/j.survophthal.2016.10.009.

629   **Chávez-Munguía B, Omaña-Molina M, González-Lázaro M, González-Robles A, Bonilla P,**

630   **Martínez-Palomo A. 2005.** Ultrastructural study of encystation and excystation in

631   *Acanthamoeba castellanii. Journal of Eukaryotic Microbiology* 52:153–158. DOI:

632   https://doi.org/10.1111/j.1550-7408.2005.04-3273.x.

633   **Cope JR, Collier SA, Nethercut H, Jones JM, Yates K, Yoder JS. 2017.** Risk behaviors for

634   contact lens–related eye infections among adults and adolescents — United States, 2016.

635   *Morbidity and Mortality Weekly Report* 66:841–845 DOI: 10.15585/mmwr.mm6632a2.

636   **Eawsakul K, Chinavinijkul P, Saeeng R, Chairoungdua A, Tuchinda P, Nasongkla N. 2017.**

637   Preparation and characterizations of RSPP050-loaded polymeric micelles using poly

638   (ethylene glycol)-*b*-poly (ε-caprolactone) and poly (ethylene glycol)-*b*-poly (D, L-lactide).

639   *Chemical Pharmaceutical Bulletin*. 65:530-537. DOI: 10.1248/cpb.c16-00871.

640   **El-Sayed NM, Hikal WM. 2015.** Several staining techniques to enhance the visibility of

641   *Acanthamoeba* cysts. *Parasitology Research* 114:823–830. DOI: 10.1007/s00436-014-4190-

642   4.

643   **Esboei BR, Fakhar M, Saberi R, Barati M, Moslemi M, Hassannia H, Dadimoghadam Y,**

644   **Jalallou N. 2020.** Genotyping and phylogenic study of *Acanthamoeba* isolates from

645   human keratitis and swimming pool water samples in Iran. *Parasite Epidemiology and*

646   *Control* 11:e00164. DOI: 10.1016/j.parepi.2020.e00164.

647   **Fakae LB, Stevenson CW, Zhu X-Q, Elsheikha HM. 2020.** *In vitro* activity of *Camellia*

648   *sinensis* (green tea) against trophozoites and cysts of *Acanthamoeba castellanii*.

649   *International Journal for Parasitology: Drugs and Drug Resistance* 13:59–72. DOI:

650   10.1016/j.ijpddr.2020.05.001.

651   **Fanselow N, Sirajuddin N, Yin X-T, Huang AJW, Stuart PM. 2021.** *Acanthamoeba* keratitis,

652   pathology, diagnosis and treatment. *Pathogens* 10:323. DOI: 10.3390/pathogens10030323.

653   **Foglieni C, Meoni C, Davalli AM. 2001.** Fluorescent dyes for cell viability: an application on

654   prefixed conditions. *Histochemistry and Cell Biology* 115:223–229. DOI:

655   10.1007/s004180100249.

656   **Harbiyeli II, Bozkurt B, Erdem E, Ozcan HG, Cam B, Sertdemir Y, Yagmur M. 2022.**

657   Associations with meibomian gland loss in soft and rigid contact lens wearers. *Contact*

658   *Lens and Anterior Eye* 45:101400 DOI: 10.1016/j.clae.2020.12.005.

659 **Heredero-Bermejo I, Copa-Patiño JL, Soliveri J, Fuentes-Paniagua E, de la Mata FJ,**

660   **Gomez R, Perez-Serrano J. 2015.** Evaluation of the activity of new cationic carbosilane

661   dendrimers on trophozoites and cysts of *Acanthamoeba polyphaga*. Parasitology

662   Research 114:473–486. DOI: 10.1007/s00436-014-4205-1.

663 **Heredero-Bermejo I, Martín-Pérez T, Copa-Patiño JL, Gómez R, de la Mata FJ, Soliveri J,**

664   **Pérez-Serrano J. 2020.** Ultrastructural study of *Acanthamoeba polyphaga* trophozoites

665   and cysts treated *in vitro* with cationic carbosilane dendrimers. *Pharmaceutics* 12:565

666   DOI: 10.3390/pharmaceutics12060565.

667 **Hidalgo E, Dominguez C. 2001.** Mechanisms underlying chlorhexidine-induced cytotoxicity.

668   Toxicology *in vitro*: *an international journal published in association with BIBRA*

669   15:271–276. DOI: 10.1016/s0887-2333(01)00020-0.

670 **International Organization for Standardization ISO 10993-5. 2009.** *Biological evaluation of*

671   *medical devices, Part 5: tests for in vitro cytotoxicity.* Geneva, Switzerland: International

672   Organization for Standardization.

673 **Kadry GM, Ismail MAM, El-Sayed NM, El-Kholy HS, El-Akkad DMH. 2021.** *In vitro*

674   amoebicidal effect of *Aloe vera* ethanol extract and honey against Acanthamoeba spp.

675   cysts. *Journal of Parasitic Diseases* 45:159–168. DOI: 10.1007/s12639-020-01292-8.

676 **Kalra SK, Sharma P, Shyam K, Tejan N, Ghoshal U. 2020.** *Acanthamoeba* and its pathogenic

677   role in granulomatous amebic encephalitis. *Experimental Parasitology* 208:107788 DOI:

678   10.1016/j.exppara.2019.107788.

679 **Kolören O, Kolören Z, Şekeroğlu ZA, Çolayvaz M, Karanis P. 2019.** Amoebicidal and

680   amoebistatic effects of *Artemisia argyi* methanolic extracts on *Acanthamoeba castellanii*

681   trophozoites and cysts. *Acta Parasitologica* 64:63–70. DOI: 10.2478/s11686-018-00009-

682   5.

683 **Kusrini E, Hashim F, Gunawan C, Mann R, Azmi WNNWN, Amin NM. 2018.** Anti-amoebic

684   activity of acyclic and cyclic-samarium complexes on *Acanthamoeba*. *Parasitology*

685   *Research* 117:1409–1417 DOI: 10.1007/s00436-018-5814-x.

686 **Kusrini E, Hashim F, Saleh MI, Adnan R, Usman A, Zakaria IN, Prihandini WW, Putra N,**

687   **Prasetyanto EA. 2020.** Monoclinic cerium (III) picrate tetraethylene glycol complex:

688   design, synthesis and biological evaluation as anti-amoebic activity against

689   *Acanthamoeba* sp. *Journal of Materials Science* 55:9795–9811. DOI: 10.1007/s10853-

690   020-04793-2.

691 **Lacerda AG de, Lira M. 2021.** *Acanthamoeba* keratitis: a review of biology, pathophysiology

692   and epidemiology. *Ophthalmic and Physiological Optics* 41:116–135 DOI:

693   https://doi.org/10.1111/opo.12752.

694 **Lee T-H, Hu C-C, Lee S-S, Chou M-Y, Chang Y-C. 2010.** Cytotoxicity of chlorhexidine on

695   human osteoblastic cells is related to intracellular glutathione levels. *International*

696   *Endodontic Journal* 43:430–435. DOI: 10.1111/j.1365-2591.2010.01700.x.

697 **Lee Y-R, Na B-K, Moon E-K, Song S-M, Joo S-Y, Kong H-H, Goo Y-K, Chung D-I, Hong**

698   **Y. 2015.** Essential role for an M17 leucine aminopeptidase in encystation of

699   *Acanthamoeba castellanii*. *PLOS ONE* 10:e0129884 DOI:

700   10.1371/journal.pone.0129884.

701 **Lee JW, Somerville T, Kaye SB, Romano V. 2021.** *Staphylococcus aureus* keratitis: incidence,

702   pathophysiology, risk factors and novel strategies for treatment. *Journal of Clinical*

703   *Medicine* 10:758. DOI: 10.3390/jcm10040758.

704 **Lorenzo-Morales J, Díaz-Marrero AR, Cen-Pacheco F, Sifaoui I, Reyes-Batlle M, Souto**

705 **ML, Hernández Daranas A, Piñero JE, Fernández JJ. 2019.** Evaluation of

706 oxasqualenoids from the red alga *Laurencia viridis* against *Acanthamoeba*. *Marine Drugs*

707 17:420. DOI: 10.3390/md17070420.

708 **Lorenzo-Morales J, Khan NA, Walochnik J. 2015.** An update on *Acanthamoeba keratitis*:

709 diagnosis, pathogenesis and treatment. *Parasite* 22:10. DOI: 10.1051/parasite/2015010.

710 **Lorenzo-Morales J, Martín-Navarro CM, López-Arencibia A, Arnalich-Montiel F, Piñero**

711 **JE, Valladares B. 2013.** *Acanthamoeba keratitis*: an emerging disease gathering

712 importance worldwide? *Trends in Parasitology* 29:181–187 DOI:

713 10.1016/j.pt.2013.01.006.

714 **Mahabusarakam W, Kuaha K, Wilairat P, Taylor WC. 2006.** Prenylated xanthones as

715 potential antiplasmodial substances. *Planta Medica* 72:912–916. DOI: 10.1055/s-2006-

716 947190.

717 **Mahabusarakam W, Proudfoot J, Taylor W, Croft K. 2009.** Inhibition of lipoprotein

718 oxidation by prenylated xanthones derived from mangostin. *Free Radical Research*.

719 33:643-659 DOI: 10.1080/10715760000301161.

720 **Marciano-Cabral F, Cabral G. 2003.** *Acanthamoeba* spp. as agents of disease in humans.

721 *Clinical Microbiology Reviews* DOI: 10.1128/CMR.16.2.273-307.2003.

722 **Marines HM, Osato MS, Font RL. 1987.** The value of calcofluor white in the diagnosis of

723 mycotic and *Acanthamoeba* infections of the eye and ocular adnexa. *Ophthalmology*

724 94:23–26. DOI: 10.1016/S0161-6420(87)33516-X.

725   **Mattar FE, Byers TJ. 1971.** Morphological changes and the requirements for macromolecule

726   synthesis during excystment of *Acanthamoeba castellanii*. *The Journal of Cell Biology*

727   49:507–519. DOI: 10.1083/jcb.49.2.507.

728   **Maycock NJR, Jayaswal R. 2016.** Update on *Acanthamoeba keratitis*: diagnosis, treatment, and

729   outcomes. *Cornea* 35:713–720. DOI: 10.1097/ICO.0000000000000804.

730   **McKelvie J, Alshiakhi M, Ziaei M, Patel DV, McGhee CN. 2018.** The rising tide of

731   *Acanthamoeba keratitis* in Auckland, New Zealand: a 7-year review of presentation,

732   diagnosis and outcomes (2009–2016). *Clinical & Experimental Ophthalmology* 46:600–

733   607 DOI: https://doi.org/10.1111/ceo.13166.

734   **Mitsuwan W, Bunsuwansakul C, Leonard TE, Laohaprapanon S, Hounkong K,**

735   **Bunluepuech K, Kaewjai C, Mahboob T, Raju CS, Dhobi M, Pereira M de L,**

736   **Nawaz M, Wiart C, Siyadatpanah A, Norouzi R, Nissapatorn V. 2020.** *Curcuma*

737   *longa* ethanol extract and curcumin inhibit the growth of *Acanthamoeba triangularis*

738   trophozoites and cysts isolated from water reservoirs at Walailak University, Thailand.

739   *Pathogens and Global Health* 114:194–204 DOI: 10.1080/20477724.2020.1755551.

740   **Momčilović S, Cantacessi C, Arsić-Arsenijević V, Otranto D, Tasić-Otašević S. 2019.** Rapid

741   diagnosis of parasitic diseases: current scenario and future needs. *Clinical Microbiology and*

742   *Infection* 25:290–309. DOI: 10.1016/j.cmi.2018.04.028.

743   **Moon E-K, Hong Y, Chung D-I, Goo Y-K, Kong H-H. 2014.** Down-regulation of cellulose

744   synthase inhibits the formation of endocysts in *Acanthamoeba*. *The Korean Journal of*

745   *Parasitology* 52:131–135 DOI: 10.3347/kjp.2014.52.2.131.

746 **Mooney R, Masala M, Martial T, McGinness C, Henriquez FL, Williams RAM. 2020.**

747 Alkyl-carbon chain length of two distinct compounds and derivatives are key

748 determinants of their anti-*Acanthamoeba* activities. *Scientific Reports* 10:1–11 DOI:

749 10.1038/s41598-020-62934-8.

750 **Nakisah MA, Ida Muryany MY, Fatimah H, Nor Fadilah, R, Zalilawati, MR, Khamsah, S,**

751 **Habsah, M. 2012.** Anti-amoebic properties of a Malaysian marine sponge *Aaptos* sp. on

752 *Acanthamoeba castellanii. World J Microbiol Biotechnol* 28:1237–1244 DOI

753 10.1007/s11274-011-0927-8.

754 **Nauman MC, Johnson JJ. 2022.** The purple mangosteen (*Garcinia mangostana*): Defining the

755 anticancer potential of selected xanthones. *Pharmacological Research* 175:106032 DOI:

756 10.1016/j.phrs.2021.106032.

757 **Neff RJ, Ray SA, Benton WF, Wilborn M. 1964.** Chapter 4 Induction of synchronous

758 encystment (differentiation) in *Acanthamoeba* sp. In: prescott DM ed. *Methods in Cell*

759 *Biology*. Academic Press, 55–83.

760 **Nielsen SE, Ivarsen A, Hjortdal J. 2020.** Increasing incidence of *Acanthamoeba keratitis* in a

761 large tertiary ophthalmology department from year 1994 to 2018. *Acta Ophthalmologica*

762 98:445–448 DOI: https://doi.org/10.1111/aos.14337.

763 **Niyyati M, Dodangeh S, Lorenzo-Morales J. 2016.** A review of the current research trends in

764 the application of medicinal plants as a source for novel therapeutic agents against

765 *Acanthamoeba* infections. *Iranian Journal of Pharmaceutical Research : IJPR* 15:893–

766 900.

767 **O·Callaghan R, Caballero A, Tang A, Bierdeman M. 2019.** *Pseudomonas aeruginosa* keratitis:

768   protease IV and PASP as corneal virulence mediators. *Microorganisms* 7:281. DOI:

769   10.3390/microorganisms7090281.

770 **Sangkanu S, Mitsuwan W, Mahabusarakam W, Jimoh TO, Wilairatana P, Girol AP,**

771   **Verma AK, de Lourdes Pereira M, Rahmatullah M, Wiart C, Siyadatpanah A,**

772   **Norouzi R, Mutombo PN, Nissapatorn V. 2021.** Anti-*Acanthamoeba* synergistic effect

773   of chlorhexidine and *Garcinia mangostana* extract or α-mangostin against *Acanthamoeba*

774   *triangularis* trophozoite and cyst forms. *Scientific Reports* 11:1–11. DOI:

775   10.1038/s41598-021-87381-x.

776 **Sangkanu S, Mitsuwan W, Mahboob T, Mahabusarakam W, Chewchanwuttiwong S,**

777   **Siphakdi P, Jimoh TO, Wilairatana P, Dolma KG, Pereira M de L, Rahmatullah M,**

778   **Wiart C, Norouzi R, Siyadatpanah A, Mutombo PN, Nissapatorn V. 2022.**

779   Phytochemical, anti-*Acanthamoeba*, and anti-adhesion properties of *Garcinia*

780   *mangostana* flower as preventive contact lens solution. *Acta Tropica* 226:106266 DOI:

781   10.1016/j.actatropica.2021.106266.

782 **Sarink MJ, van der Meijs NL, Denzer K, Koenderman L, Tielens AGM, van Hellemond JJ.**

783   **2022.** Three encephalitis-causing amoebae and their distinct interactions with the host.

784   *Trends in Parasitology* 38:230–245 DOI: 10.1016/j.pt.2021.10.004.

785 **Shing B, Balen M, Debnath A. 2021.** Evaluation of amebicidal and cysticidal activities of

786   antifungal drug isavuconazonium sulfate against *Acanthamoeba* T4 Strains.

787   *Pharmaceuticals* 14:1294. DOI: 10.3390/ph14121294.

788   **Ting DSJ, Ho CS, Deshmukh R, Said DG, Dua HS. 2021.** Infectious keratitis: an update on

789   epidemiology, causative microorganisms, risk factors, and antimicrobial resistance. *Eye*

790   *(London, England)* 35:1084–1101. DOI: 10.1038/s41433-020-01339-3.

Figure 1

The chemical structures of semi-synthetic mangostin derivatives.

C1 named 1,3-Dihydroxy-6-(2,3-epoxypropoxy)-7-methoxy-2,8-bis(3-methylbut-2-enyl)-9H-xanthen-9-one, C2 named 1-Hydroxy-3,6-di(4-cyanopropoxy)-7-methoxy-2,8-bis(3-methylbut-2-enyl)-9H xanthen-9-one, and C3 named 1,3-Dihydroxy-6-(4-cyanopropoxy)-7-methoxy-2,8-bis(3-methylbut-2-enyl)-9H-xanthen-9-one.
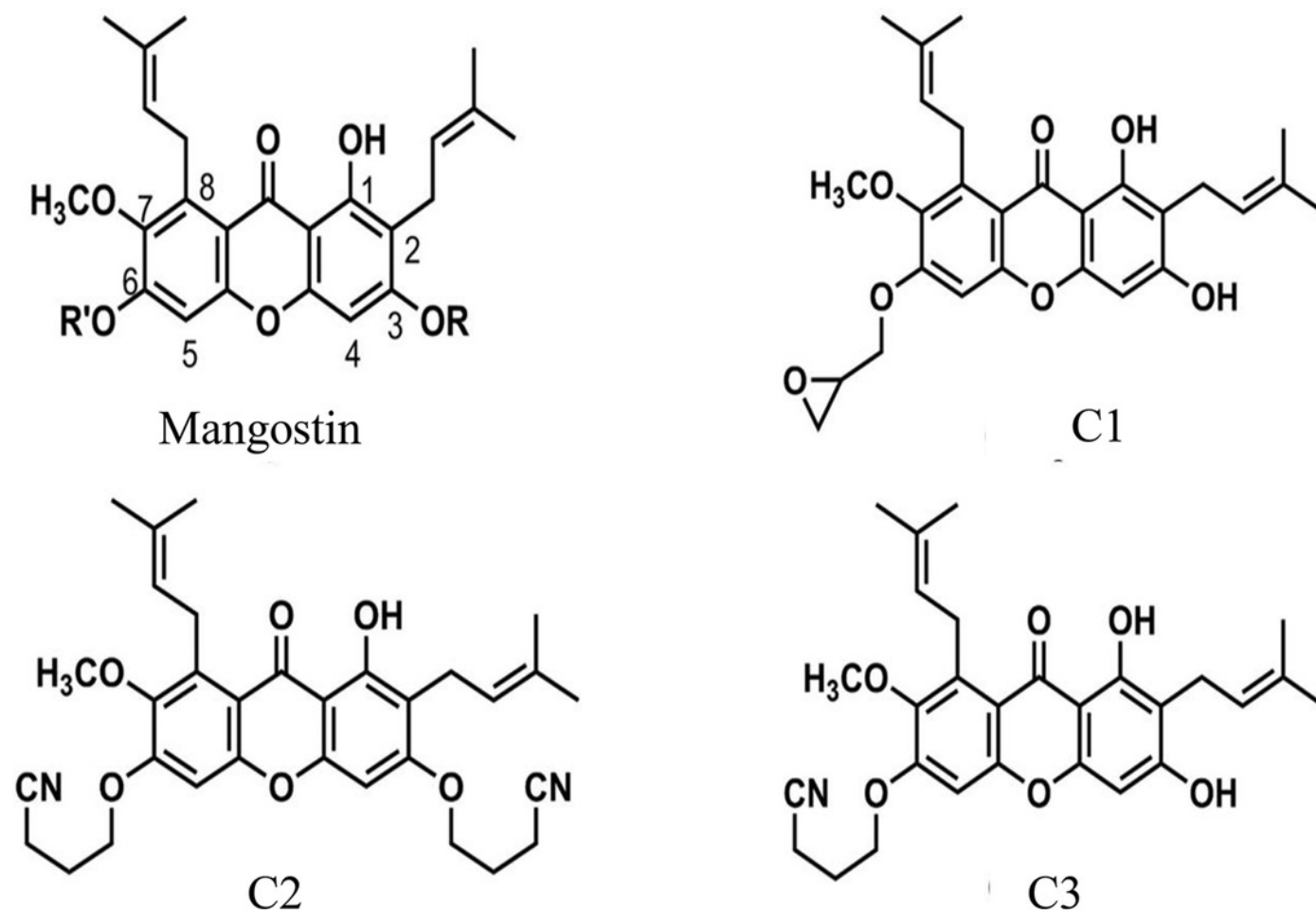
Figure 2

Identification of mangostin derivative (C1) IC_{50} and chlorhexidine (CHX) IC_{50}.

(A) and (B) are representative images of C1 IC_{50} towards trophozoites and cysts, respectively. (C) and (D) are representative images of CHX IC_{50} towards trophozoites and cysts, respectively. Values are presented as mean ± standard deviation (SD) of triplicate determinations (*n* = 3).
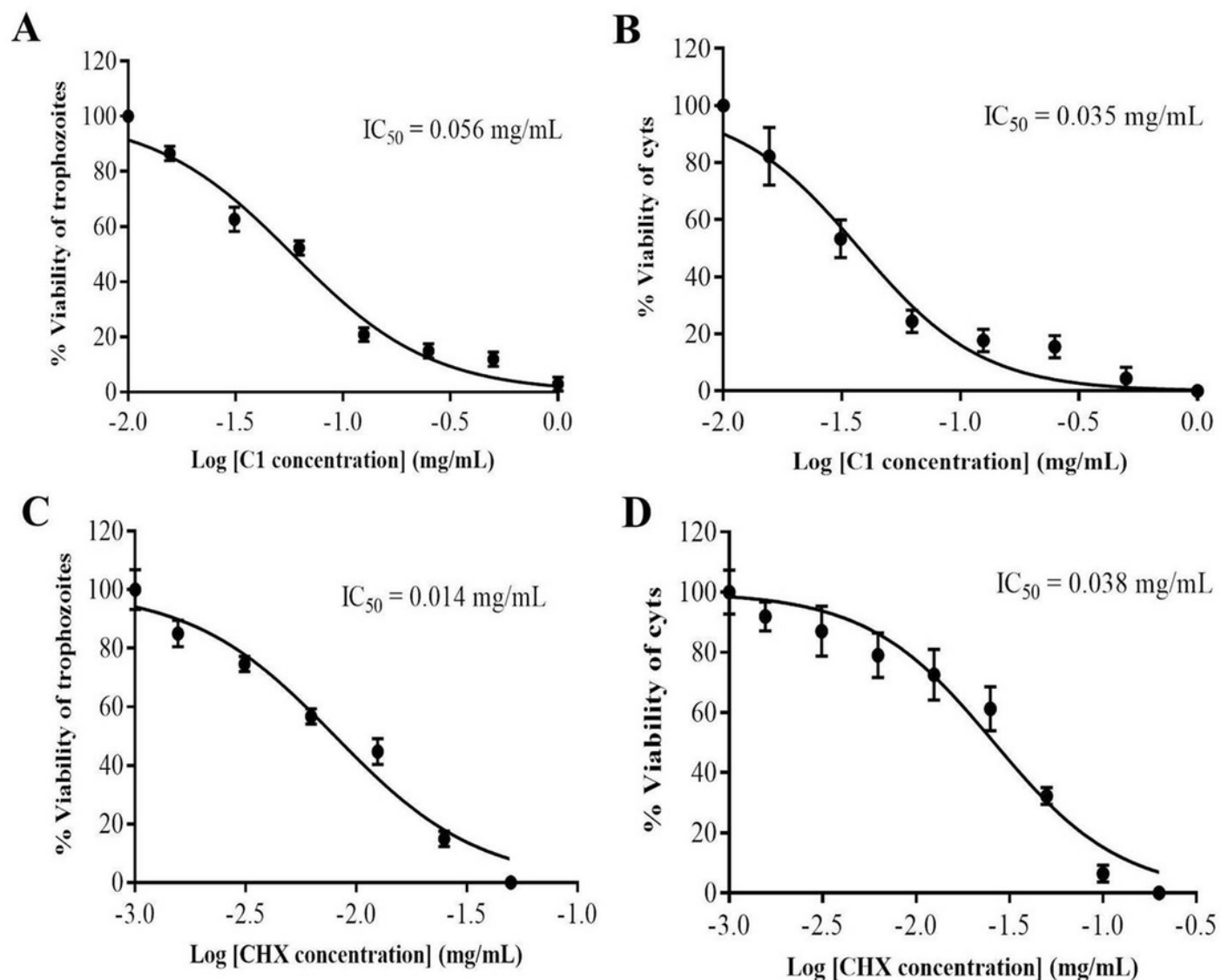
Figure 3

Morphological changes of *Acanthamoeba triangularis* trophozoites after exposure to mangostin derivative (C1).

(A-C) Treated cell with 1/2 MIC C1. (D-F) Treated cells with 1/2 ×MIC chlorhexidine (CHX) and (G-I) treated cells with 1% (v/v) DMSO. CHX and DMSO were used as positive and negative controls, respectively. Morphological changes of the *A. triangularis* were observed by SEM. Magnifications were revealed as: A, D, G = 5,000X; D, E, F = 10,000X; G, H, I = 30,000X.
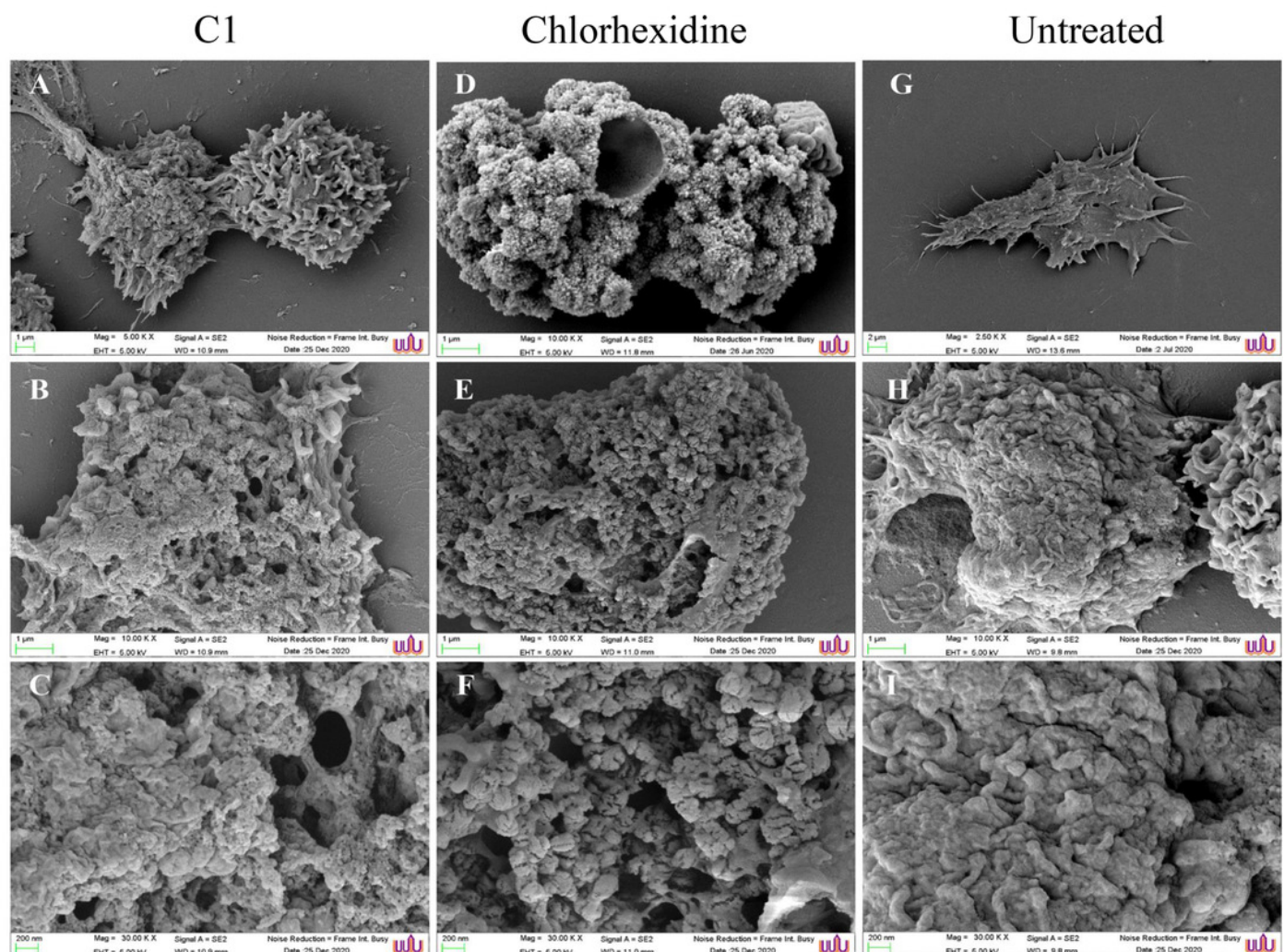
Figure 4

Morphological changes of *Acanthamoeba triangularis* cysts after exposure to mangostin derivative (C1).

(A-C) Treated cell with 1/2×MIC C1. (D-F) Treated cell with 1/2×MIC chlorhexidine (CHX) and (G-I) treated cell with 1% (v/v) DMSO. CHX and DMSO were used as positive and negative controls, respectively. Morphological changes of *A. triangularis* were observed by SEM. Magnifications were revealed as: A, D, G = 5,000X; D, E, F = 10,000X; G, H, I = 30,000X.
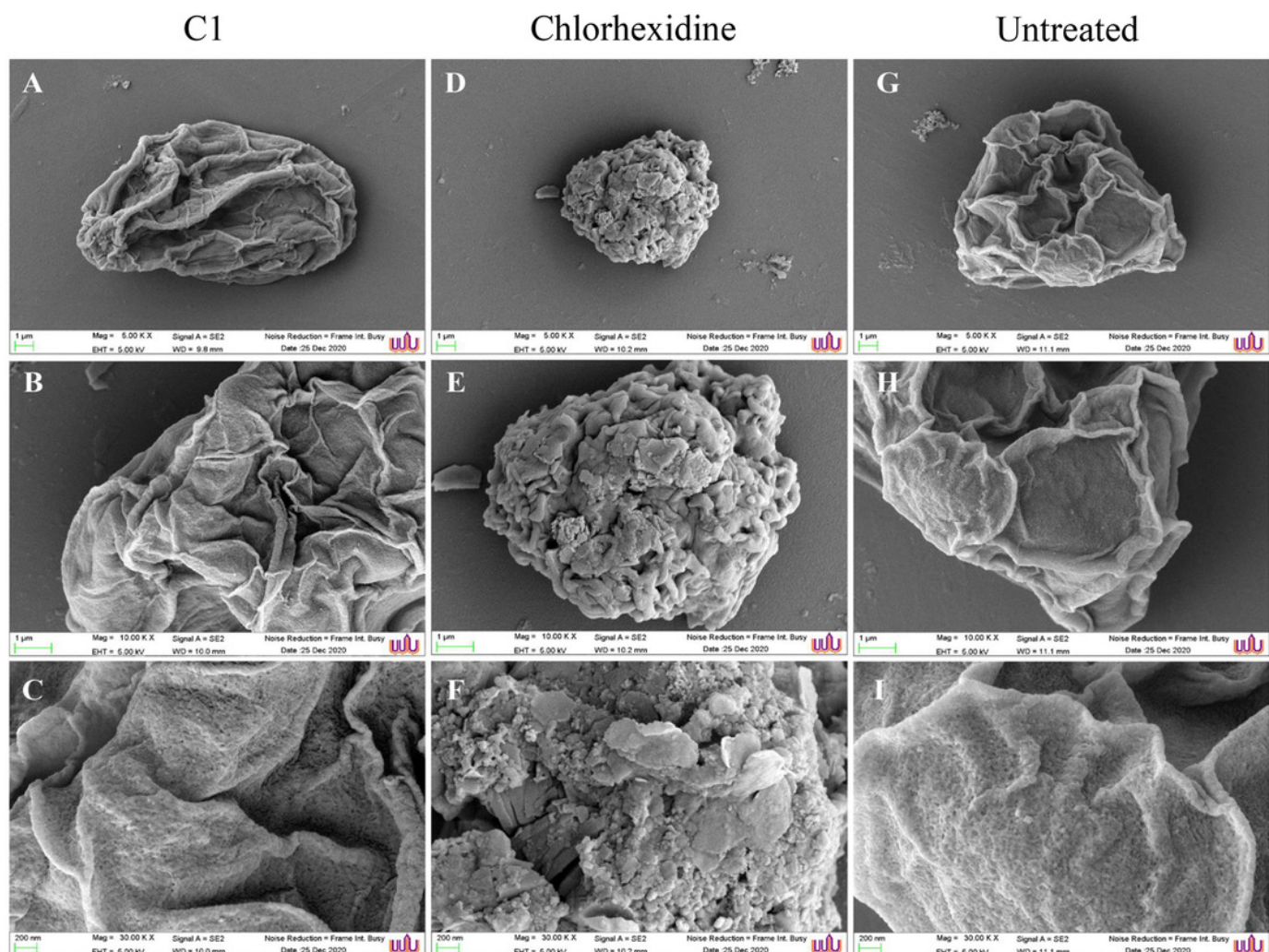
Figure 5

Representative images of *Acanthamoeba triangularis* trophozoites stained with AO/PI dye under fluorescent microscopy.

(A) Treat cells with 1/2×MIC value of mangostin derivative (C1). (B) Treated cells with 1/2×MIC value of chlorhexidine (CHX). (C) Untreated cells.
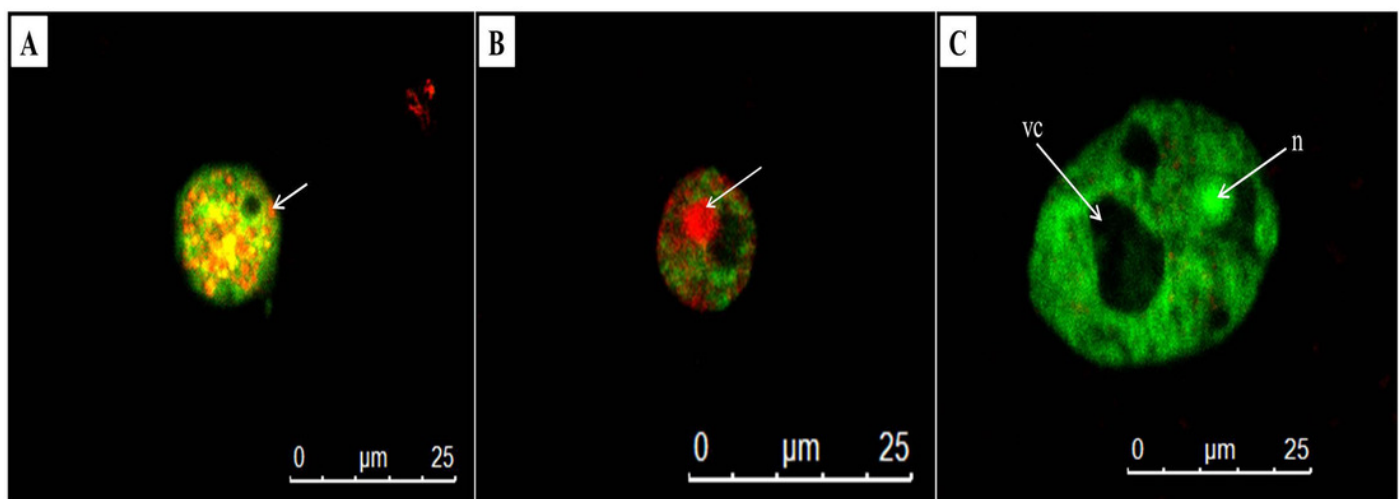
Figure 6

Acanthamoeba triangularis cysts stained with Calcofluor white (CFW) dye under fluorescent microscopy.

(A) Cyst-specific staining with CFW dye under light microscope. (B) Healthy cyst-specific staining using CFW dye under fluorescent microscope. (C) Treated cysts with 1/2×MIC value of mangostin derivative (C1) and stained with CFW dye under fluorescent microscope. (D) Treated cells with 1/2×MIC value of chlorhexidine (CHX) and stained with CFW dye under fluorescent microscope. (E) Untreated cysts and stained with CFW dye under fluorescent microscope. Magnifications were revealed as: A, B = 1,000X; C, D, E = 400X.
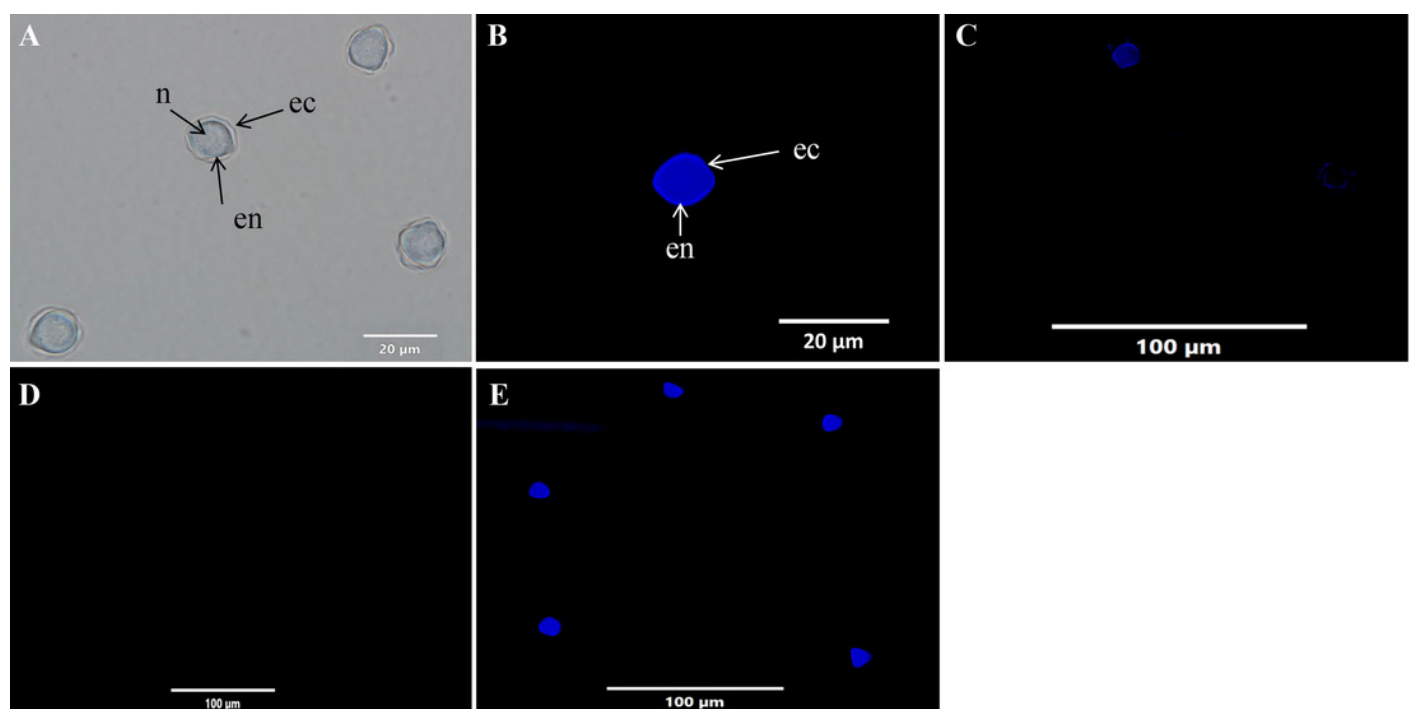
Figure 7

In vitro cytotoxic effect of mangostin derivative (C1) and chlorhexidine (CHX) against Vero cells.

The cytotoxic activity of C1 (A and B) and CHX (A) on Vero cells was evaluated after incubation at 37 °C for 24 h.
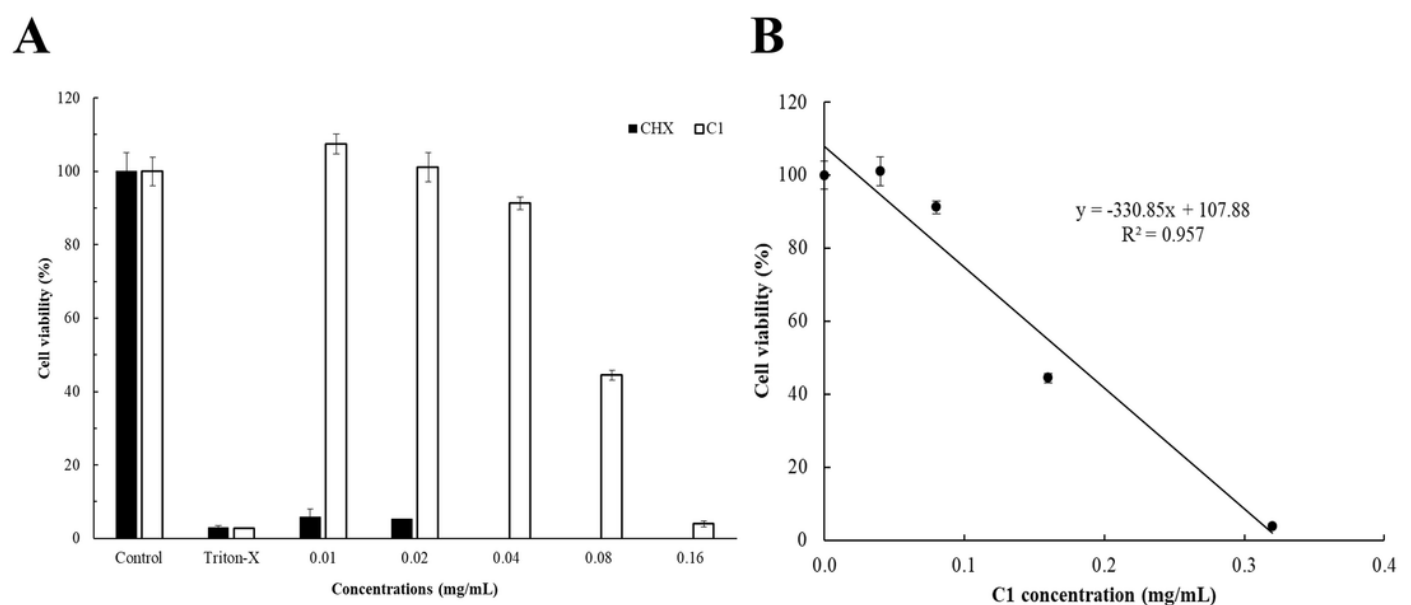
Figure 8

Inhibition of *Acanthamoeba triangularis* encystation by mangostin derivative (C1).

Inhibition encystation of *A. triangularis* after exposure to different MIC values of C1, 10 mM PMSF and without any agent (untreated; control) for 72 h. Bars represent the standard deviation (SD) (n = 3). *p < 0.05, statistically significant difference. Images of the encystation inhibition were observed by inverted microscope (200X) after exposure to C1 at 1/16×MIC, 10 mM PMSF, and without any agent (untreated; control) for 72 h.
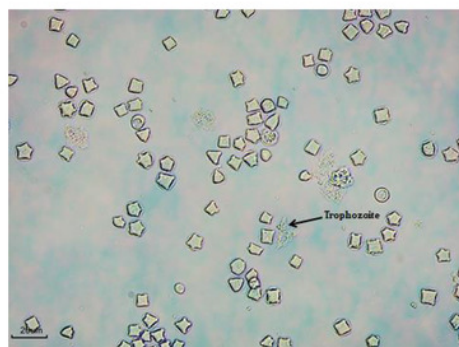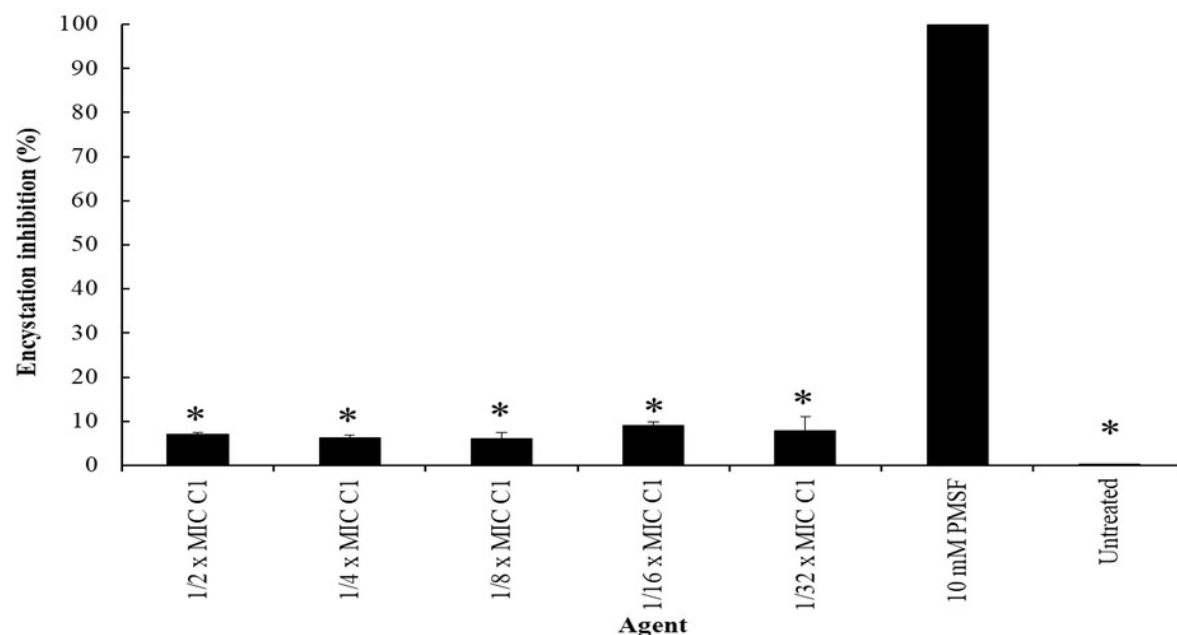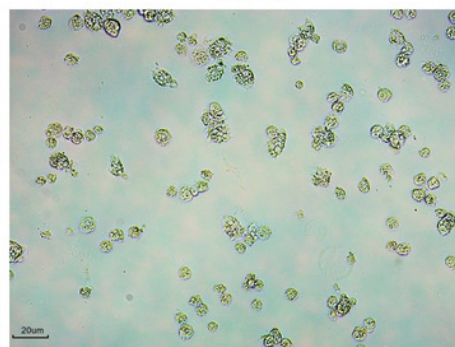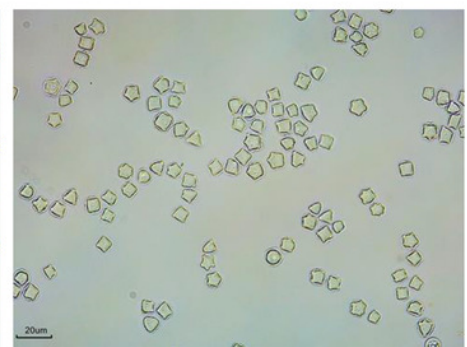
Figure 9

Excystation activity of *Acanthamoeba triangularis* by mangostin derivative (C1).

Excystation rates of *A. triangularis* after exposure to different MIC values of C1, 10 mM PMSF, and without any agent (untreated; control) for 7 days. Values are presented as mean ± standard deviation (SD) of triplicate determinations ($n = 3$). *$p < 0.05$, statistically significant difference. Images of the excystation were observed by inverted microscope (200X) after exposure to C1 at 1/128 × MIC, 10 mM PMSF for 7 days, and without any agent (untreated; control) for 7 days and 10 days.
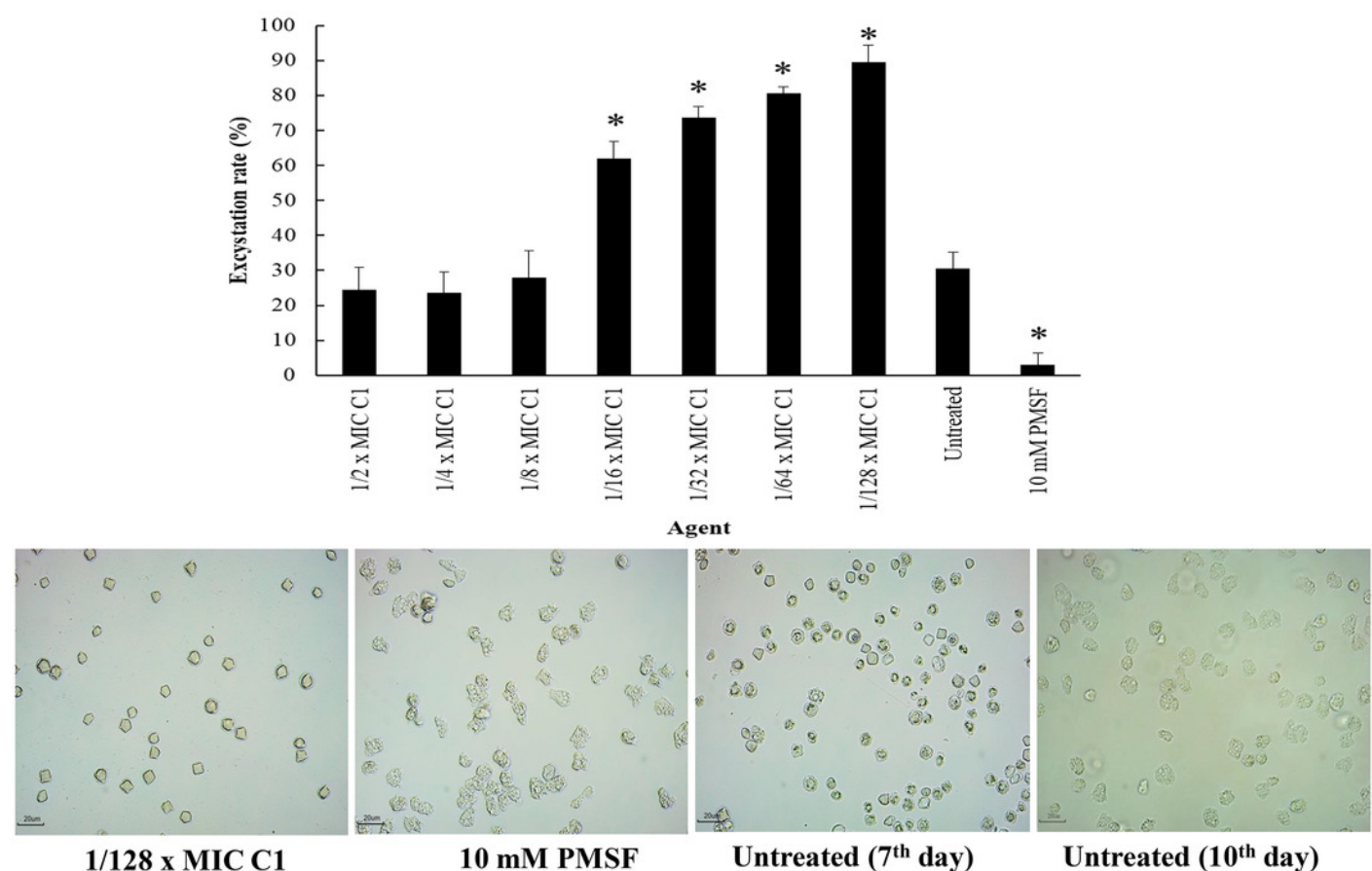
Figure 10

The number of *Acanthamoeba triangularis* on contact lenses after treatment with chlorhexidine, MPD-1 (Renu®freshTM), MPD-2 (Duna NO RUB), and C1.

(A) Adhesive trophozoites and (B) cysts in removal test. The adhesive cells were counted using an inverted microscope. Values are presented as mean ± standard deviation (SD) of triplicate determinations (n = 3). *p < 0.05, statistically significant difference.
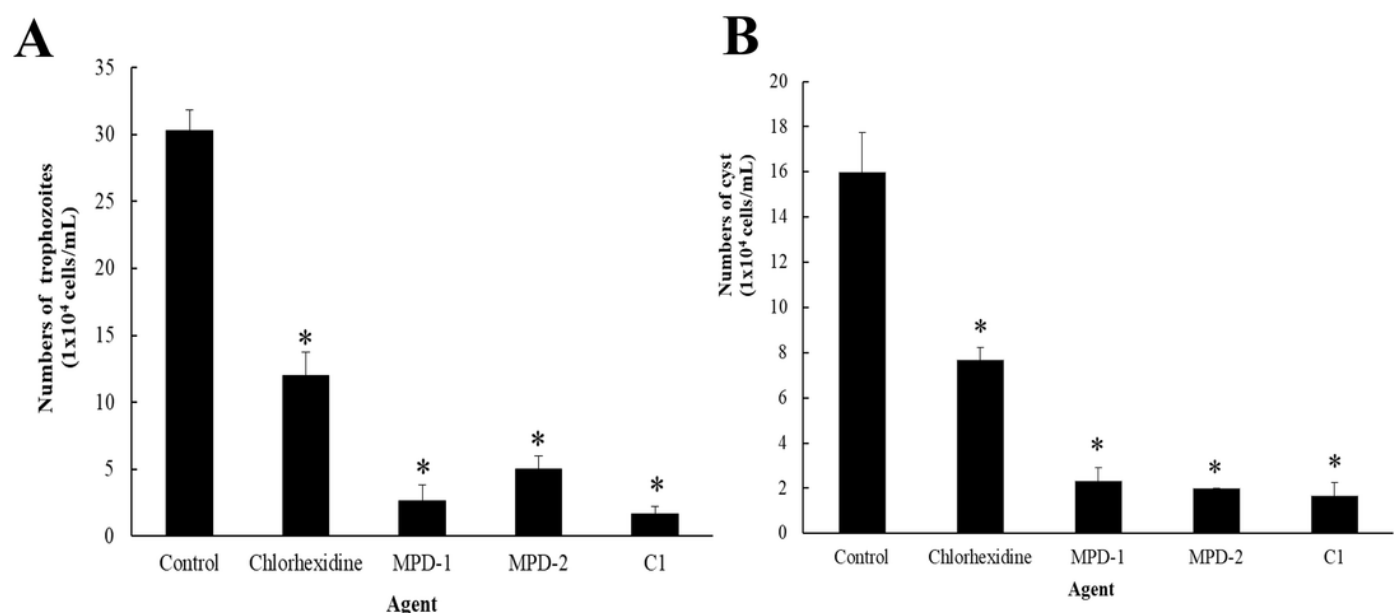
Screening of anti-*Acanthamoeba* activity and minimal inhibitory concentration (MIC) of semi-synthetic mangostin derivatives and chlorhexidine against *A. triangularis* WU19001 trophozoites and cysts.

Symbol: +, positive with inhibition of more than 90% of viable growth compared with the control.

1 **Table 1:**

2 Screening of anti-*Acanthamoeba* activity and minimal inhibitory concentration (MIC) of semi-

3 synthetic mangostin derivatives and chlorhexidine against *A. triangularis* WU19001 trophozoites

4 and cysts.

Anti-*Acanthamoeba* agent	Anti-*Acanthamoeba* activity at a final concentration of 1 mg/mL		MIC (mg/mL)	
	Trophozoite	Cyst	Trophozoite	Cyst
C1	+	+	0.128	0.064
C2	+	+	0.512	1.024
C3	+	+	0.512	1.024
Chlorhexidine	+	+	0.016	0.064

5 Symbol: +, positive with inhibition of more than 90% of viable growth compared with the
6 control.